

**Project Report  
ATC-55**

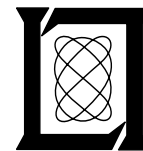
# **The Logan MLS Multipath Experiment**

D.A. Shnidman

23 September 1975

---

**Lincoln Laboratory**  
MASSACHUSETTS INSTITUTE OF TECHNOLOGY  
*LEXINGTON, MASSACHUSETTS*



Prepared for the Federal Aviation Administration,  
Washington, D.C. 20591.

This document is available to the public through  
the National Technical Information Service,  
Springfield, VA 22161

This document is disseminated under the sponsorship of the Department of Transportation in the interest of information exchange. The United States Government assumes no liability for its contents or use thereof.

1. Report No. FAA-RD-75-130		2. Government Accession No.		3. Recipient's Catalog No.	
4. Title and Subtitle The Logan MLS Multipath Experiment				5. Report Date 23 September 1975	
				6. Performing Organization Code	
7. Author(s) D. A. Shnidman				8. Performing Organization Report No. ATC-55	
9. Performing Organization Name and Address Massachusetts Institute of Technology Lincoln Laboratory P. O. Box 73 Lexington, Massachusetts 02173				10. Work Unit No. (TRAIS)	
				11. Contract or Grant No. DOT-FA74WAI-461	
				13. Type of Report and Period Covered Project Report	
12. Sponsoring Agency Name and Address Department of Transportation Federal Aviation Administration Systems Research and Development Service Washington, D.C. 20591				14. Sponsoring Agency Code	
15. Supplementary Notes The work reported in this document was performed at Lincoln Laboratory, a center for research operated by the Massachusetts Institute of Technology under Air Force Contract F19628-76-C-0002.					
16. Abstract  The National Plan for a Microwave Landing System (MLS) has specified a carrier frequency for the system in the vicinity of 5.1 GHz. At that frequency, no multipath data taken at a major civilian airport existed. The purpose of this experiment was to obtain such data at Logan International Airport in order to ascertain: 1) which objects are the major causes of measurable multipath reflections and their levels relative to the direct signal (M/D level), 2) whether or not the reflections from these objects can be satisfactorily simulated by the Lincoln computer model and, if so, how complicated must that model be, and 3) if the characteristics of multipath provide a significant discriminant between the Doppler and scanning beam techniques.  It was found in the experiment that regions where reflections were noted could be predicted from ray optics and diffraction. No measurable reflections were noted elsewhere. For the purpose of modeling for multipath, building surfaces could be characterized as a flat plate with a reflection coefficient determined by measurement if it were a complicated surface, or by the dielectric properties of the surface material, if a simple surface. The airplane reflection model was also found to agree well with measurements.					
17. Key Words Microwave Landing System C-band multipath			18. Distribution Statement Document is available to the public through the National Technical Information Service, Springfield, Virginia 22151.		
19. Security Classif. (of this report) Unclassified		20. Security Classif. (of this page) Unclassified		21. No. of Pages 88	

## ACKNOWLEDGMENT

The author is indebted to James E. Evans for his many useful suggestions and comments on both the experiment and this document and to Massport for its cooperation, without which the experiment would not have been possible.

## TABLE OF CONTENTS

<u>Section</u>		<u>Page</u>
I	INTRODUCTION	1
II	DESCRIPTION OF THE TEST EQUIPMENT	3
	2.1 Physical Description	3
	2.2 Transmitted Signals	3
	2.3 The ITS Channel Sounder	7
	2.4 Antennas	11
III	LOGAN INTERNATIONAL AIRPORT	14
IV	EXPERIMENTAL DESIGN CONSIDERATIONS	17
	4.1 Lincoln Multipath Model	17
	4.2 Location of Reflecting Objects	22
	4.3 Experiment Geometries	24
V	EXPERIMENTAL RESULTS	26
	5.1 Pier C Area Multipath	26
	5.2 Pier B Multipath	36
	5.3 International Terminal Building	36
	5.4 Delta Hangar	44
	5.5 NAFEC Data	52
	5.6 Airplane Multipath	55
	5.7 Ground Reflections	71
VI	DISCRIMINATION BETWEEN DOPPLER AND SCANNING BEAM MLS	78
VII	CONCLUSIONS	80
	REFERENCES	81

## LIST OF ILLUSTRATIONS

<u>Figure</u>	<u>Title</u>	<u>Page</u>
1	FAA Modified Cortez Van with Mast Down	4
2	Transmitter Trailer and Pickup Truck	5
3	Transmitter Dish Antenna on Tractor	6
4	Channel Sounder Transmitter Block Diagram	8
5	Sample of Waveform and Correlation Function	9
6	Channel Sounder Receiver Block Diagram	10
7	Measured Horizontal Pattern of 6-Foot Dish	12
8	Horn Antenna Pattern	13
9	Aerial Photograph of Logan Airport	15
10	General Location Plan of Logan Airport	16
11	Experiment Transmitter and Receiver Locations	18
12	Possible Ray Paths for Vertical Structure Ground Reflections	21
13	Reflection Ellipse	23
14	Ground Lobing for 11 December 1974 Data	25
15	Pier C	27
16	Geometry For 24 October 1974	29
17	Channel Sounder Processed Output for 24 October 1974	30
18	Geometry for 9 December 1974	33
19	Comparison of 9 December 1974 Data with Model M/D Levels	34
20	The Volpe International Terminal	37
21	Geometry for the International Terminal	40

List of Illustrations (cont'd)

<u>Figure</u>	<u>Title</u>	<u>Page</u>
22	Geometry for Runway 15R Multipath From International Terminal	42
23	The Delta Hangar	45
24	Geometry for 8 December 1974	46
25	Comparison of Lower Antenna Pulsed Data and cw Data	48
26	Comparison of 8 December 1974 Data with Multipath Model M/D Results	49
27	Rear of NAFEC Hangar Building No. 301	53
28	Geometry for NAFEC, 7 October 1974	54
29	Comparison of 7 October 1974 Data with Multipath Model M/D Results	56
30	Location of Aircraft, Transmitters, and Receivers for Airplane Multipath Experiments	58
31	Geometry for 12 December 1974 Boeing 747 Mast Run	59
32	Comparison of 12 December 1974 Data with Multipath M/D Results	63
33	Boeing 747 Airplane	64
34	Geometry for 11 December 1974 Boeing 747 Experiment	65
35	Comparison of 11 December 1974 Data with B747 Multipath Model M/D Results	66
36	Boeing 727 Airplane	67
37	Geometry for 12 December 1974 Boeing 727 Experiment	69
38	Comparison of 12 December 1974 Data with B727 Multipath Model M/D Results	70
39	cw Strip Chart from 18 October 1974	72
40	Geometry for 25 October 1974 B747 Experiment	75
41	cw Strip Chart from 25 October 1974 B747 Experiment	76

## THE LOGAN MLS MULTIPATH EXPERIMENT

### I. INTRODUCTION

The National Plan for a Microwave Landing System (MLS) has specified a carrier frequency for the system in the vicinity of 5.1 GHz. At that frequency, no multipath data taken at a major civilian airport existed. The purpose of this experiment was to obtain such data at Logan International Airport in order to ascertain: (1) which objects are the major causes of measurable multipath reflections and their levels relative to the direct signal (M/D level), (2) whether or not the reflections from these objects can be satisfactorily simulated by the Lincoln computer model<sup>[1]</sup> and, if so, how complicated must that model be, and (3) if the characteristics of multipath provide a significant discriminant between the Doppler and scanning beam techniques.

A joint effort, sponsored by the FAA, was undertaken by M.I.T. Lincoln Laboratory and the Institute for Telecommunication Sciences (ITS), Boulder, Colorado. ITS would provide the means of taking and processing the data and Lincoln Laboratory would guide the experiment and analyze the processed data. The data were taken during two periods, from 17 October 1974 to 26 October 1974, and from 8 December 1974 to 13 December 1974.

It was found that regions where reflections were noted could be predicted from the locations of the transmitter, receiver, and large reflecting object by means of geometrical optics and diffraction. No measurable reflections were noted elsewhere. For the purposes of multipath reflections, buildings could generally be classified into one of two categories: (1) buildings with complex surfaces (broken by columns, jetways, etc.) and low reflections, and (2) buildings with simple surfaces. For both, the model is a plate that concurs (in size) with the dimensions of the building. For the latter case, the reflection coefficient is determined from the dielectric property of the building surface material while for the former case, the reflection coefficient is chosen to be commensurate with peak measured M/D levels and not related to the construction material. This was due to the fact that the complicated surfaces generally broke up the reflected signal, thereby reducing the M/D levels

significantly below that which would be expected for a homogeneous plate, while not producing measurable reflections elsewhere. Reflections from airplanes were also studied and utilized to improve and verify the aircraft models used for multipath computations.

The multipath levels observed from the runway locations were generally low enough such that both techniques (Doppler and TRSB), which were under consideration in the U.S. MLS program, should perform adequately, i.e., there were no multipath characteristics in the "realistic geometry" measurements on the runways that would obviously yield a discriminant between Doppler and TRSB.

## II. DESCRIPTION OF THE TEST EQUIPMENT

The important features of the test equipment are described in this section.

### 2.1 Physical Description

The receiver equipment was housed in a 22-foot, FAA modified Cortez van (Fig. 1) equipped with an adjustable mast. By means of the mast, the receiver antennas could be raised or lowered to any desired height (from 0 to 50 feet, for the lower antennas, and from 20 to 70 feet for the antenna on the top of a 20-foot fiberglass extension pole). The van was equipped with a 115-volt generator, which provided power for the equipment.

The transmitter equipment was housed in a 12-foot trailer towed by a pickup truck (Fig. 2). The transmitter antenna, a 6-foot parabolic dish, was mounted on a pole on the rear of a tractor (Fig. 3). A diesel generator that provided power for the transmitter equipment was attached to the tractor. The antenna could be easily turned a full 360° by rotating the pole. It was also possible to adjust, to a limited extent, the upward tilt of the antenna.

With the above arrangement, all equipment was highly portable and, when necessary, it was possible to evacuate a runway position in less than 10 minutes.

### 2.2 Transmitted Signals

Two signals were transmitted. One was a 4.835 GHz carrier wave (cw) signal and the other a sequence of 6.67 nsec pulses on a 5.1 GHz carrier. Both signals were vertically polarized. The cw signal was used to monitor the experiment and, when only a single multipath reflection occurred, the levels can be compared to the pulsed data. The pulsed data allowed for a fine resolution of reflections so that multiple reflections can be separated and delay path differences determined as will be described in the next sections.



Fig. 1 FAAmodified Cortez van with mast down.

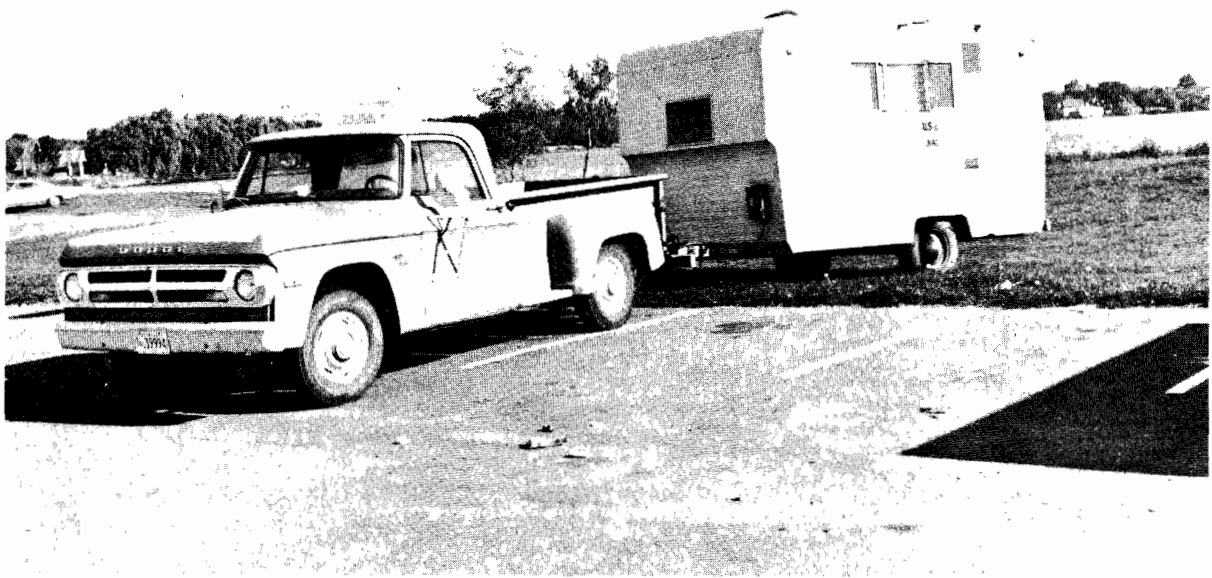


Fig. 2 Transmitter trailer and pickup truck.

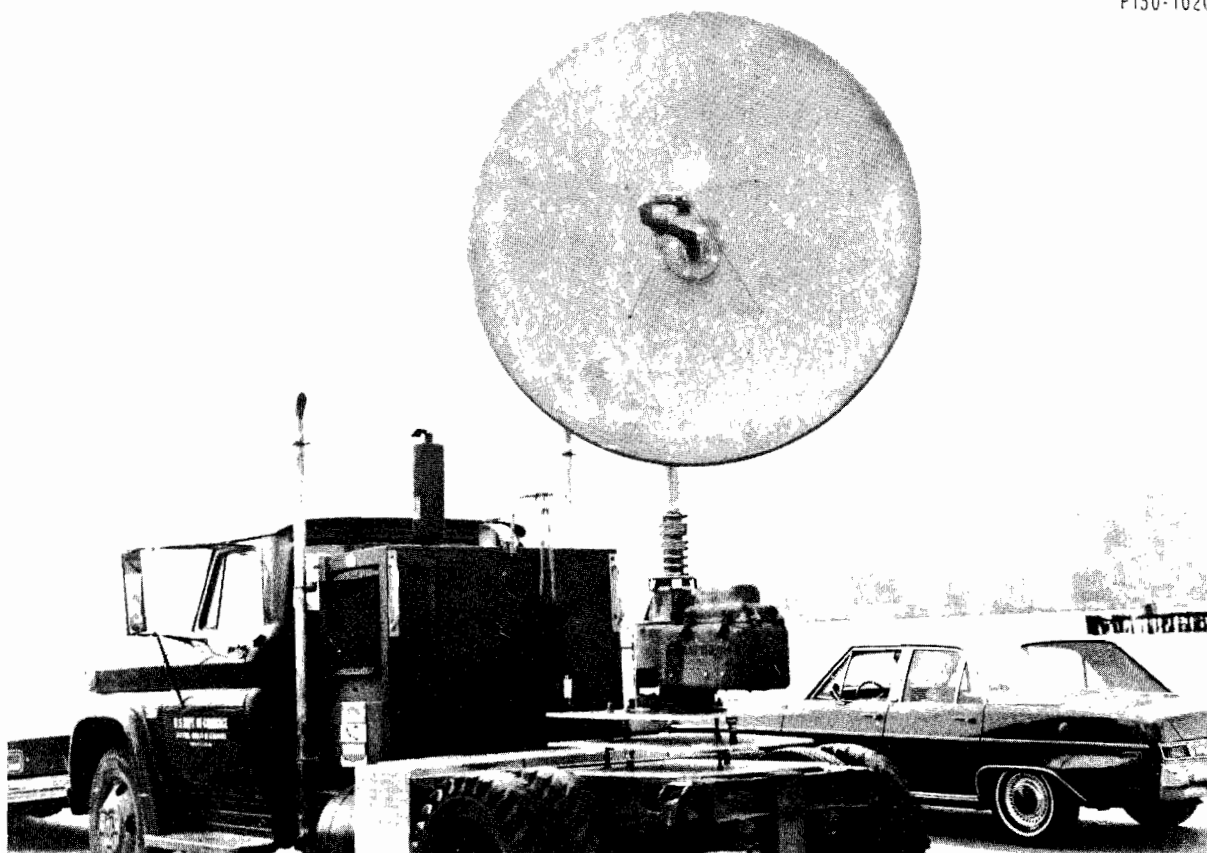


Fig. 3 Transmitter dish antenna on tractor.

### 2.3 The ITS Channel Sounder

The main instrument, which was used to gather high resolution data, was the equipment that ITS refers to as the channel sounder<sup>[2]</sup>. Designed for separating signals with path differential as small as six feet, it allowed us to determine if multiple reflections existed and, if so, the timing differences between them.

The transmitter block diagram is illustrated in Fig. 4. The PN generator delivers a 511-maximal-length sequence<sup>[3]</sup> of binary digits which are phase coded onto a carrier of 5.1-GHz for transmission. The correlation function of such a sequence is illustrated in Fig. 5 where  $\tau$  is equal to  $T$ , the chip duration. For a bit rate,  $R_T$ , of 150 M bits/sec,  $T = 6.67$  nsec. This is pulse compression by phase coded wave similar to that which is under study for L-band DME by ITT avionics<sup>\*[4]</sup>.

The receiver block diagram is illustrated in Fig. 6. If the channel sounder had been designed for a fixed sequence and chip width, then a tapped delay line or a shift-register could have been used as a matched filter. Instead, in order to allow for easy adaptation to a large variety of different length sequences and chip widths, the matched filtering is achieved by using a PN generator at the receiver with the identical sequence as that of the transmitter and correlating the received signal with this sequence. The reception is phase incoherent and both in-phase and quadrature-phase channels are correlated with the output of the PN generator. There is one key difference in that the rate,  $R_R$ , at which this sequence is generated is  $R_R = 149.985$  M bits/sec; consequently, it takes the receiver about 0.3407 nsec longer than the transmitter to complete a sequence. Because of this difference, the two sequences are continually shifting with respect to one another and come into near alignment only for one short period (approximately  $133 \frac{1}{3}$  nsec) every 10,000 repetitions of the 511-bit sequence (which takes 34.07 msec). The resulting output of the

---

\*Another implementation of pulse compression is the linear FM (or chirp) waveform proposed for the MLS DME by Texas Instruments [5].

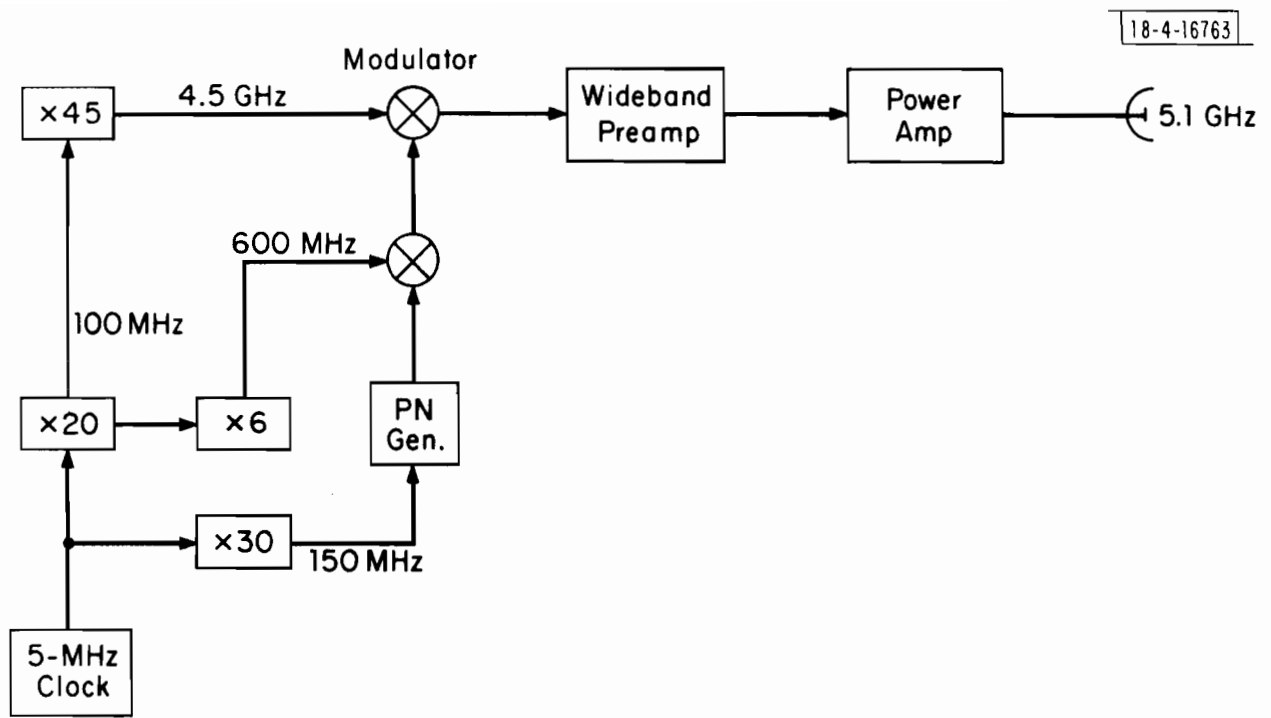
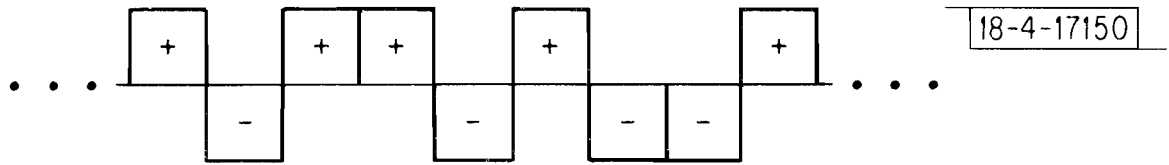
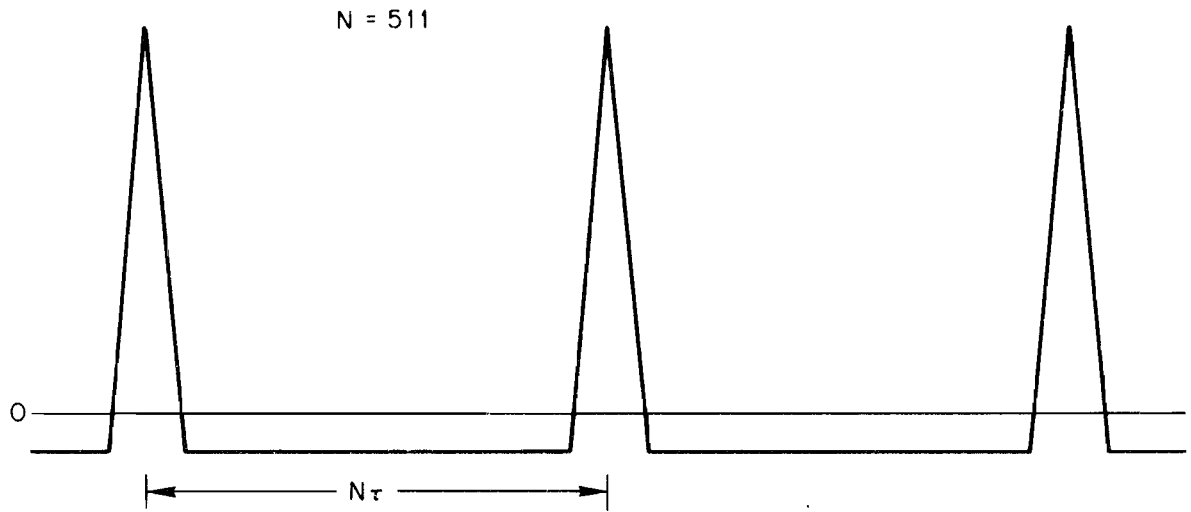


Fig. 4 Channel sounder transmitter block diagram.

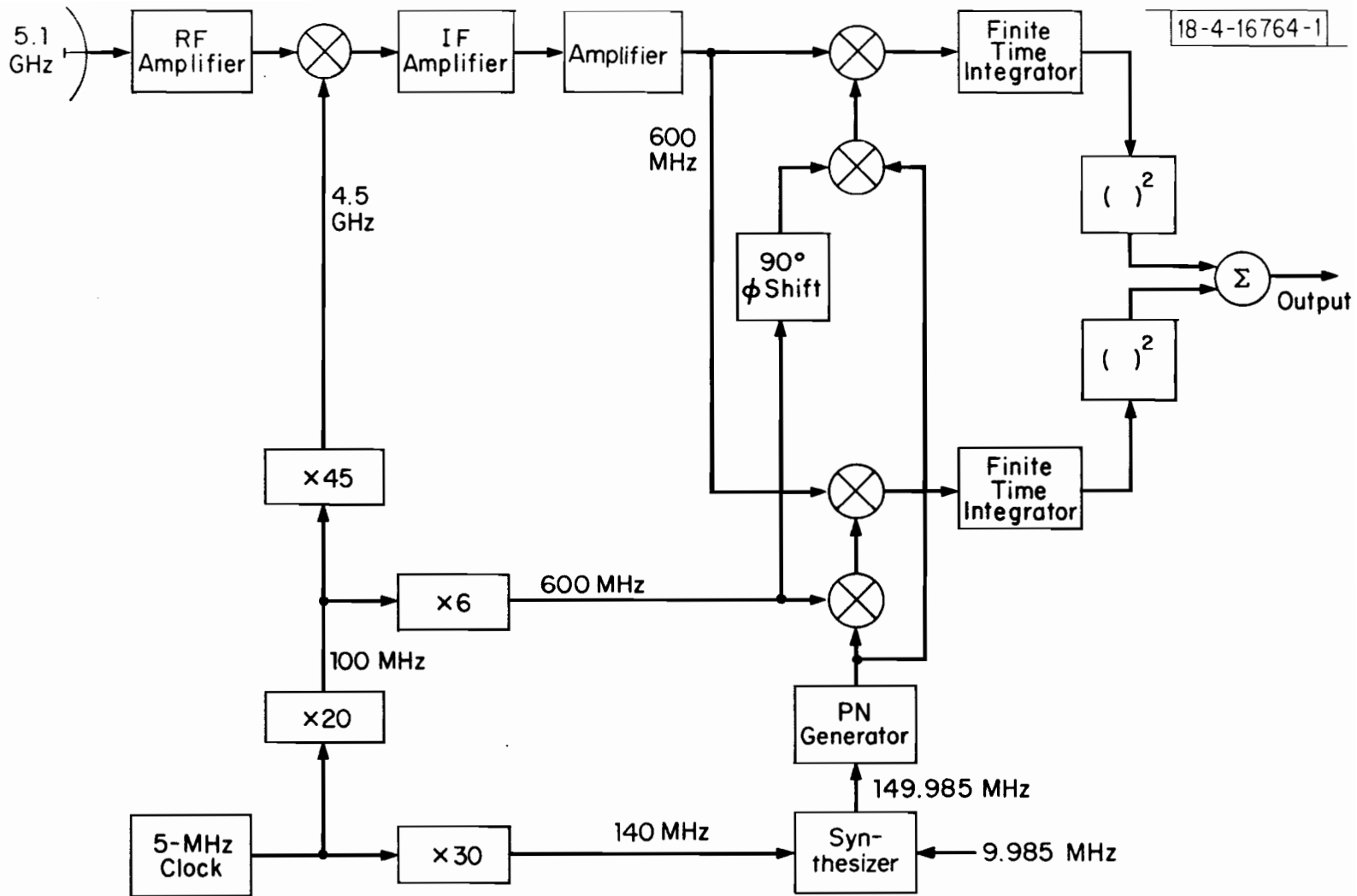


(a) PHASE CODED WAVEFORM



(b) CORRELATION FUNCTION

Fig. 5 Sample of waveform and correlation function.



RECEIVER CONFIGURATION FOR CHANNEL SOUNDER

Fig. 6 Channel sounder receiver block diagram.

receiver has the form indicated in Fig. 5 where  $\tau = 10,000T = 66.67 \mu\text{sec}$  so that the time between peaks is  $N\tau = 34.07 \text{ msec}$ . If more than one signal is received, then each would have an output similar to Fig. 5 and the total output would be the quadrature addition of each. The separation,  $\tau_j$ , between peaks within a single  $N\tau$  interval would be proportional to the path differential,  $\Delta R_j$ . If we let  $c =$  velocity of light in free space ( $9.8425 \times 10^8$  feet/sec), then

$$\Delta R_j = c \times 10^{-4} \tau_j$$

where  $\tau_j$  is in seconds.

#### 2.4 Antennas

The transmitter antenna was chosen with two considerations in mind. First, ground reflections had to be controlled to approximately the same extent as that projected for azimuth antennas, and second, good angular resolution to aid in determining the causes of multipath was important. To satisfy these two requirements, a six-foot parabolic dish antenna with a 3-dB beamwidth of  $2^\circ$  was used for the transmitter antenna. It was nominally tilted up at an angle of  $1.6^\circ$  above the horizon to reduce ground reflections. The measured horizontal antenna pattern of the dish is illustrated in Fig. 7. It was estimated that, with the  $1.6^\circ$  tilt, the rolloff of the beam pattern at the horizon was about 10 dB per degree.

In order to allow for a large angular visibility at the receiver, a broad beamwidth horn antenna was used. The receiver horn antenna pattern is illustrated in Fig. 8. The horns used for the cw receiver and upper pulsed data receiver were aimed directly to the rear of the van. The lower pulsed data antenna was mounted so as to be angled at  $30^\circ$  toward the reflecting object in order to add an additional  $30^\circ$  visibility to that side.

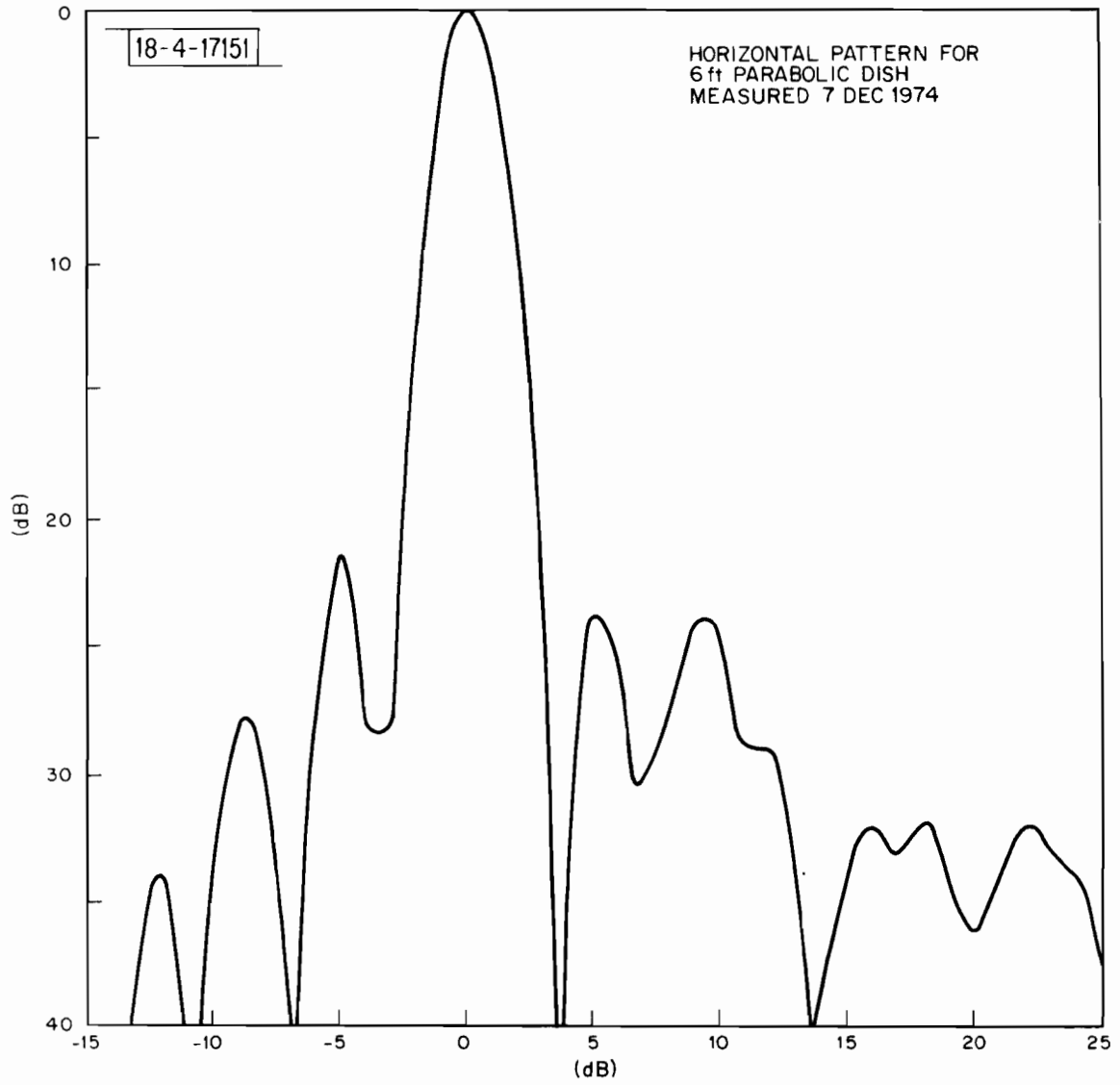


Fig. 7 Measured horizontal pattern of 6-foot dish.

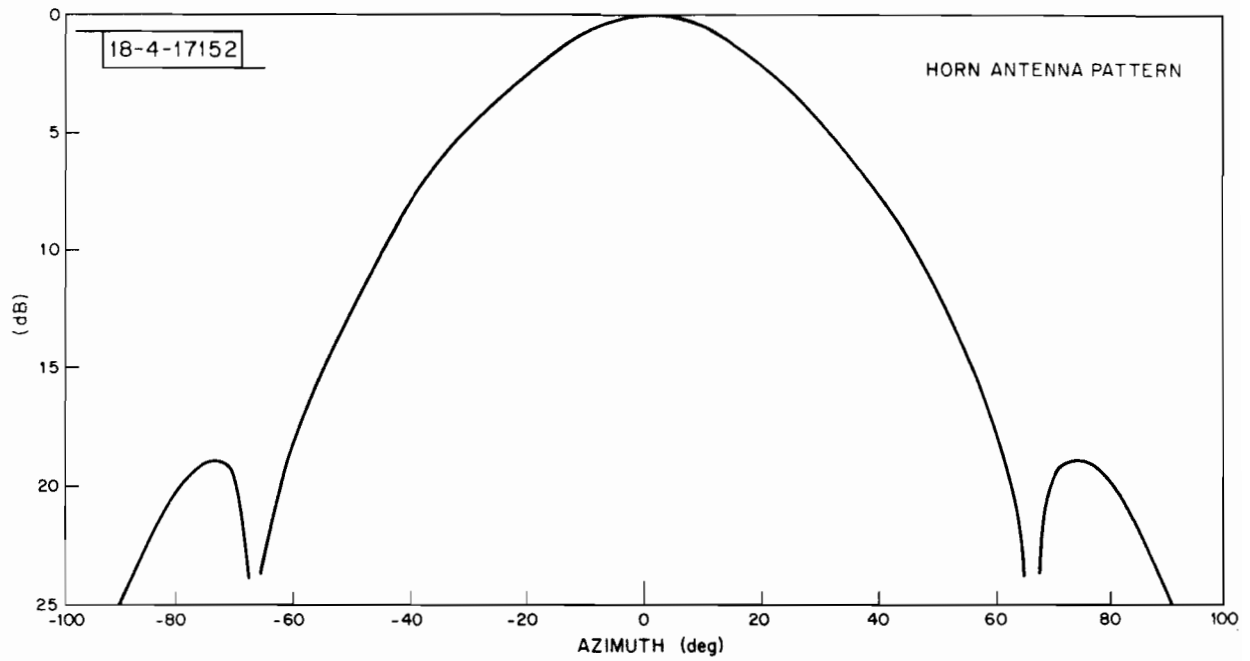


Fig. 8 Horn antenna pattern.

### III. LOGAN INTERNATIONAL AIRPORT

With the cooperation of Massport, which owns and operates Logan International Airport, and the Logan FAA controllers, we were given access to the surface of Logan Airport for the purpose of obtaining the multipath data. The arrangement was that each day we would inquire regarding which runway(s), if any, was available for our experiment. We would then have Massport officially close the runway. If a shift in wind or weather necessitated the use of that runway, we were prepared to evacuate it in less than 15 minutes. During the course of the experiment, we had access to every runway of interest.

An aerial photograph of Logan Airport is presented in Fig. 9 and a general location plan in Fig. 10. The Volpe International Building, Pier B and Pier C, (buildings 29, 31, and 33, respectively, in Fig. 10) were the only buildings that were found to cause measurable reflections for transmitter and receiver locations on the runways. There were no hangars located that would yield reflections for transmitter/receiver locations on the runways, consequently measurements were taken off the Delta hangar (building 21, Fig. 10) with the transmitter and receiver located in the North taxiway area.

Logan Airport afforded access to many airplanes, including commonly used types of wide bodied jets. With the cooperation of several airlines (especially TWA, United, and American airlines), multipath data were taken for B747s, B727s and DC-10s. (The DC-10 pulsed data were not processed for the most part and are, therefore, not included in this report.) Eastern and Delta airlines have L1011s, but time limitations prevented us from obtaining data for them.



Fig. 9 Aerial photograph of Logan Airport.

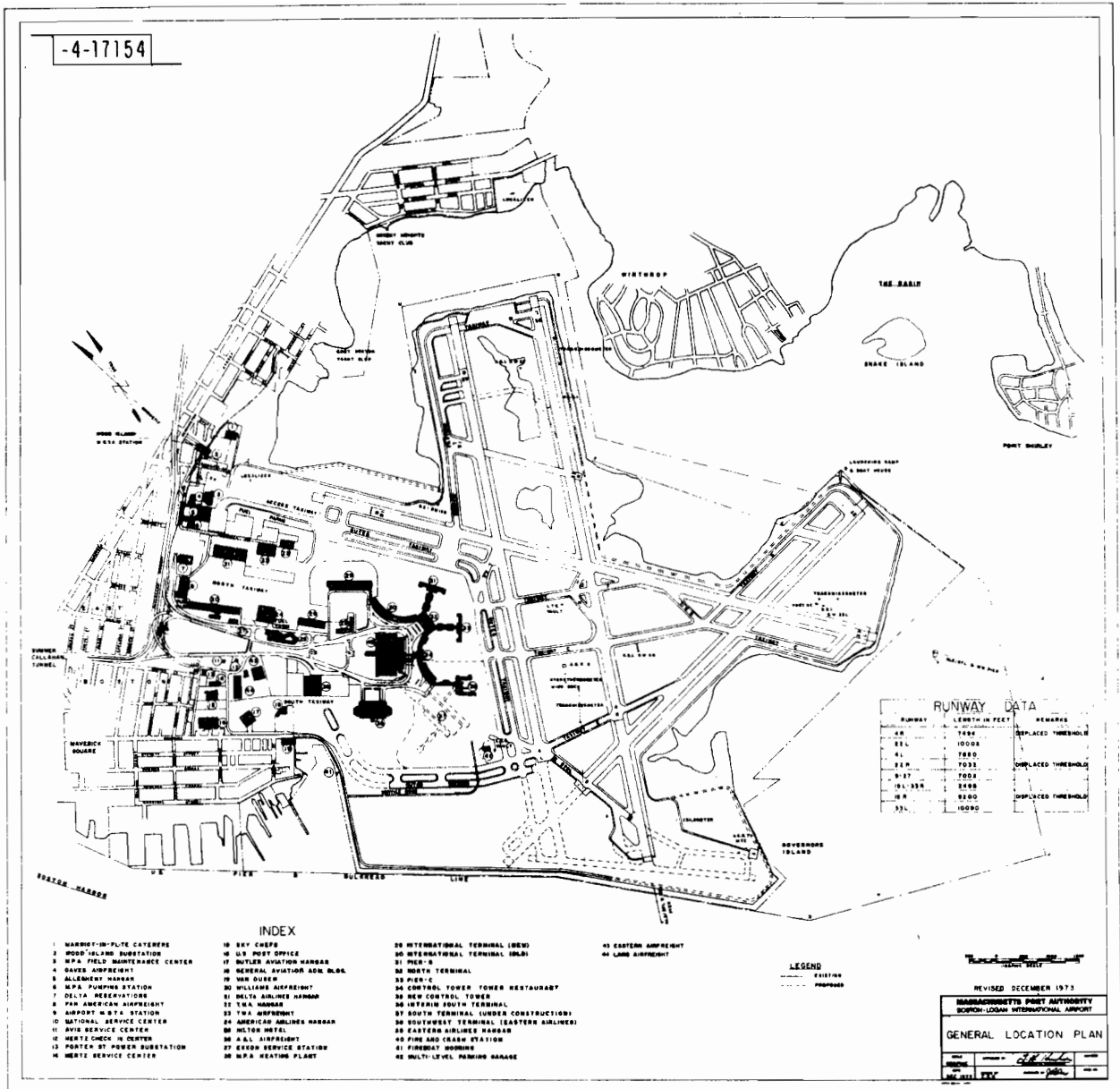


Fig. 10 General location plan of Logan Airport.

#### IV. EXPERIMENTAL DESIGN CONSIDERATIONS

One of the main purposes for this experiment is to test the validity of the Lincoln Laboratory multipath model. A verified analytical model is a powerful tool that can be used to help characterize multipath from any environment. The model also helps to provide a structure for interpreting and understanding the results of an experiment. A concise description of the Lincoln multipath model is given in Section 4.1. A second key purpose is to acquire data representative of actual multipath that a system may generate.

In considering the above, we performed two types of experiments: (1) simulation of reflections that might occur in a real MLS system, and (2) obtaining data that can be readily compared to the multipath simulation models. The geometries in the former case were comparable to those that would be found at an airport, while those in the latter usually involved much smaller distances than would arise in practice. Most of the transmitter and receiver locations used for building multipath experiments are indicated in Fig. 11.

##### 4.1 Lincoln Multipath Model

The mathematical model used for the computer simulation of reflections has been described by Jack Capon<sup>[1]</sup>. The model considers scattering from several different sources:

- (1) The ground
- (2) Buildings and hangars
- (3) Parked aircraft
- (4) Diffuse scattering from the ground
- (5) Shadowing caused by runway humps, and
- (6) Shadowing caused by aircraft approaching line of sight.

The ground reflection model is based on the Fresnel-Kirchoff integral. The physical model for a building surface scattering is one (or several) flat

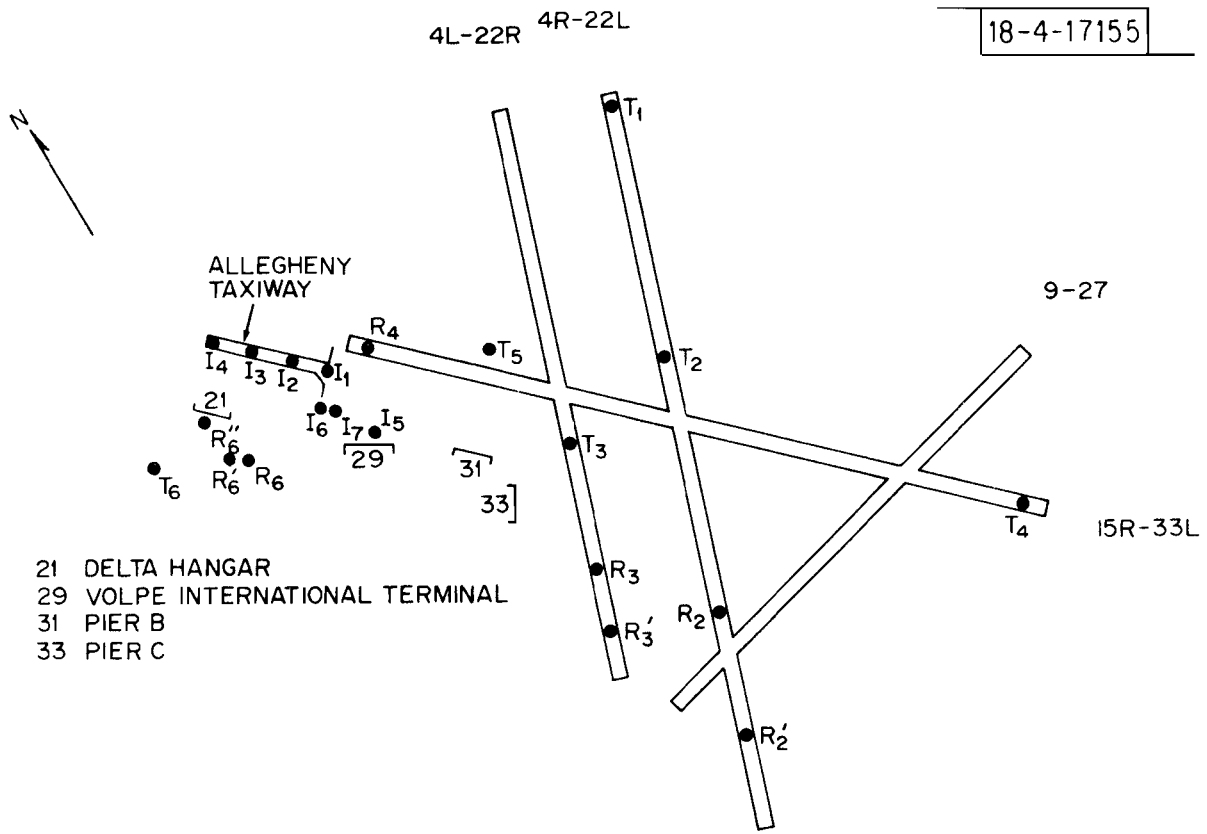


Fig. 11 Experiment transmitter and receiver locations.

plate with suitable dielectric and roughness properties. Scattering from a flat plate is then determined by using the method of images and Fresnel diffraction theory.

Aircraft fuselages are physically modeled by cylinders with tail fins treated as sections of cylinders mounted back to back. The scattering from these cylinders is calculated much like the building scattering with the addition of a divergence factor to account for the surface curvature.

The Logan Airport experiments were primarily concerned with the aforementioned items (1) through (3).

Some key parameters, in the Fresnel diffraction theory used, are  $r_0$ , the distance from transmitter to receiver,  $r_1$ , the distance from transmitter to reflecting object,  $r_2$ , the distance from reflecting object to the receiver, and  $R_f$ , the radius of the first Fresnel zone.  $R_f$  is defined by the equation

$$R_f = \sqrt{\lambda R_0}$$

where

$$R_0 = \frac{r_1 r_2}{r_1 + r_2}$$

and  $\lambda$  is the carrier wavelength ( $\lambda = 0.1930$  feet for a 5.1-GHz carrier and  $\lambda = 0.2036$  feet for a 4.835-GHz carrier).  $R_f$  can be used to estimate the size of surface area involved in determining the reflection level from an object. The smaller  $R_f$  is, the smaller the area that must be modeled in order to compare measurement with simulated results. For this reason, the smaller geometries (i.e., smaller  $r_1$  and/or  $r_2$ ) make the comparison easier.

The multipath to direct ratio (M/D) for a single reflecting surface (e.g., plate, fuselage or tail fin) is given by

$$M/D = \frac{\sum_{i=1}^4 \rho_i e^{j\phi_i}}{1 + \rho_g e^{j\phi_g}} \quad (1)$$

The ground reflection,  $\rho_g$ , of the direct path from transmitter to receiver is calculated by means of the Fresnel-Kirchoff integral. This is done to allow for changes in the reflection coefficient of the ground, as may be experienced in going from paved runway to grass, and changes in the parameters,  $r_1$  and  $r_2$ , over the reflecting surface. The four reflection paths,  $\rho_i$  ( $i=1, \dots, 4$ ), are from the transmitter to object to receiver ( $i=1$ ), from transmitter to ground to object to receiver ( $i=2$ ), from transmitter to object to ground to receiver ( $i=3$ ), and the path with both ground bounces ( $i=4$ ). These paths are illustrated in Fig. 12.

Each  $\rho_i$  is composed of several factors

$$\rho_i = \rho_R \rho_{FZ} \rho_{RC} \rho_D g_i A_T(\theta_1, \phi_1) A_R(\theta_2, \phi_2) \quad (2)$$

where

$$\rho_R = \frac{r_0}{r_1 + r_2} \quad (\text{the distance factor})$$

$\rho_{FZ}$  = the Fresnel zone factor

$\rho_{RC} = \rho_{AF} \rho_P$  where  $\rho_{AF}$  and  $\rho_P$  are described below

$\rho_D$  = a divergence factor if object is not flat [6]

$$g_i = \begin{cases} 1 & i=1 \\ \rho_{gi} & i=2,3 \\ \rho_{gi}^2 & i=4 \end{cases}$$

where  $\rho_{gi}$  = ground reflection coefficient for multipath

$\left. \begin{matrix} A_T(\theta_1, \phi_1) \\ A_R(\theta_2, \phi_2) \end{matrix} \right\} = \text{transmitter and receiver antenna patterns}$

$\theta_i, \phi_i$  ( $i=1,2$ ) = azimuth and elevation angles, respectively.

The term,  $\rho_{AF}$ , is the attenuation factor and is specified by [1]

$$\rho_{AF} = e^{-\frac{1}{2} \left[ \frac{4\pi}{\lambda} \sigma_h \cos \theta_t \right]^2} \quad (3)$$

18-4-17156

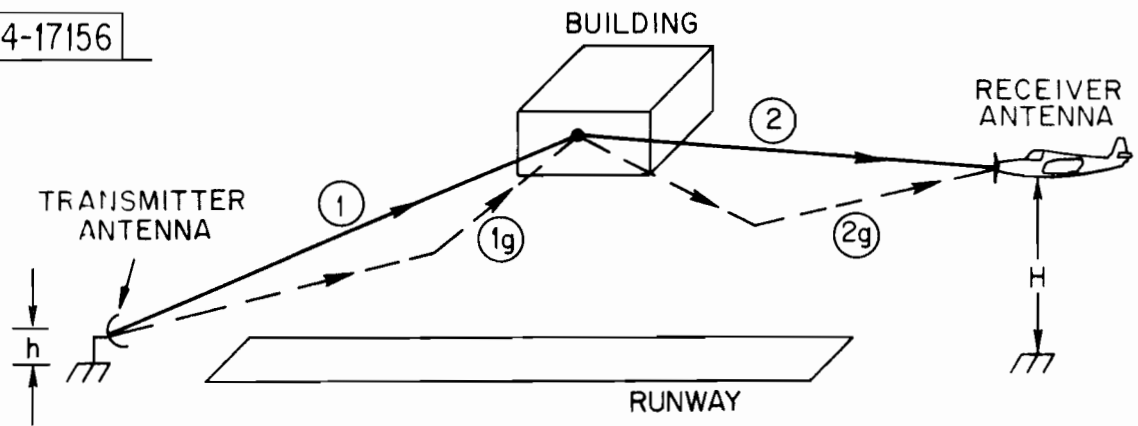


Fig. 12 Possible ray paths for vertical structure ground reflections.

where

$\theta_t$  = the angle of incidence

$\sigma_h$  = the root-mean-square roughness height.

The second factor,  $\rho_p$ , is the Fresnel reflection coefficient given in Kerr<sup>[7]</sup>, p. 396.

If the ground reflection levels are small enough to be ignored, then

$$|M/D| \approx \rho_1 .$$

For larger geometries, however, this will not necessarily be the case and ground reflections may influence some measured levels. With a measurement antenna pattern rolloff similar to MLS arrays, these measured levels should correspond to levels that will be found "in practice."

#### 4.2 Location of Reflecting Objects

For the pulsed data taken with the channel sounder, path differentials between direct and reflected signals can be determined. Using this differential,  $\Delta R$ , we have that

$$R \stackrel{\Delta}{=} r_1 + r_2 = r_0 + \Delta R .$$

We also know that the reflecting object is on an ellipse (Fig. 13) whose focal points are the transmitter and receiver locations. The major axis,  $2a$ , is equal to  $R$  and the minor axis,  $2b$ , is given by

$$2b = \sqrt{R^2 - r_0^2} .$$

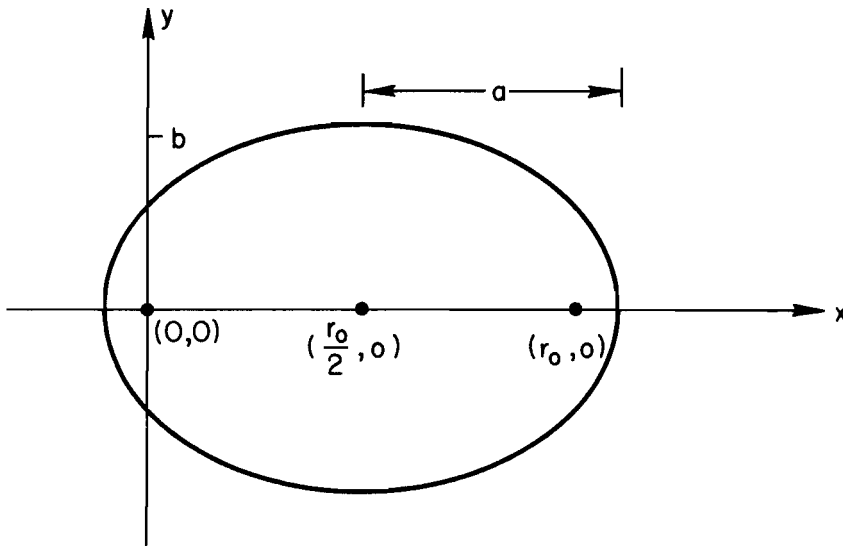
Combining this information with the angle at which the parabolic dish\* is pointing allows for fairly accurate determination of the position of the reflecting object.

The locations of the transmitter and receiver were both known to within approximately 15 feet so that  $r_0$  can be estimated to within 30 feet. Locations were generally determined by noting positions relative to some marking on the

---

\*From Fig. 7, we see that the dish has a  $2^\circ$  beamwidth between the -3 dB points.

THE TRANSMITTER IS AT  $(0,0)$  AND RECEIVER AT  $(r_0, 0)$



$r_0$  = DIRECT PATH LENGTH

$R$  = REFLECTION PATH LENGTH

EQUATION OF ELLIPSE IS

$$\frac{(x - \frac{r_0}{2})^2}{a^2} + \frac{y^2}{b^2} = 1$$

WHERE

$$a = \frac{R}{2}$$

$$b = \frac{\sqrt{R^2 - r_0^2}}{2}$$

Fig. 13 Reflection ellipse.

runway or some object which could be located on the aerial photograph of the airport or on the airport map.

As a check on the accuracy of receiver and transmitter location, we can consider some data taken on 11 December 1974 in which ground reflections were inadvertently included. For a run in which the receiving height is varied, the scalloping in the direct signal is dependent on the transmitter and receiver separations,  $r_0$ , the transmitter antenna height  $h$ , and the wavelength  $\lambda$ . In terms of  $\Delta H$ , the receiver height change between scalloping peaks,  $r_0$  is given by

$$r_0 = \frac{2h \Delta H}{\lambda} .$$

The estimate of  $r_0$  from airport photo/taxiway markings was 910 feet. The plot of the scalloping data is shown in Fig. 14 where it is estimated that  $\Delta H = 8.75$  feet. Since  $h = 10$  feet and  $\lambda = 0.1930$  feet, then by this data  $r_0 \approx 907$  feet.

### 4.3 Experiment Geometries

The locations of the transmitter and receiver for each of the combinations used in the Logan Airport experiment are indicated in Fig. 11 wherein the transmitter sites are designated by the symbols,  $T_i$ ,  $i=1, \dots, 6$  and the corresponding receiver sites by  $R_i$ ,  $i=2, 3, 4$ , and 6. When more than one receiver site was used for the same  $i$ , primes are employed. For  $i=1$ , the receiver was moved the entire length of the runway and for  $i=5$  there were numerous receiver sites for measuring reflections off the International Terminal; consequently they are designated by  $I_1, \dots, I_7$ . The salient features of each have been translated onto graph paper, as was also done with the aircraft experiment geometries, and will be presented subsequently.

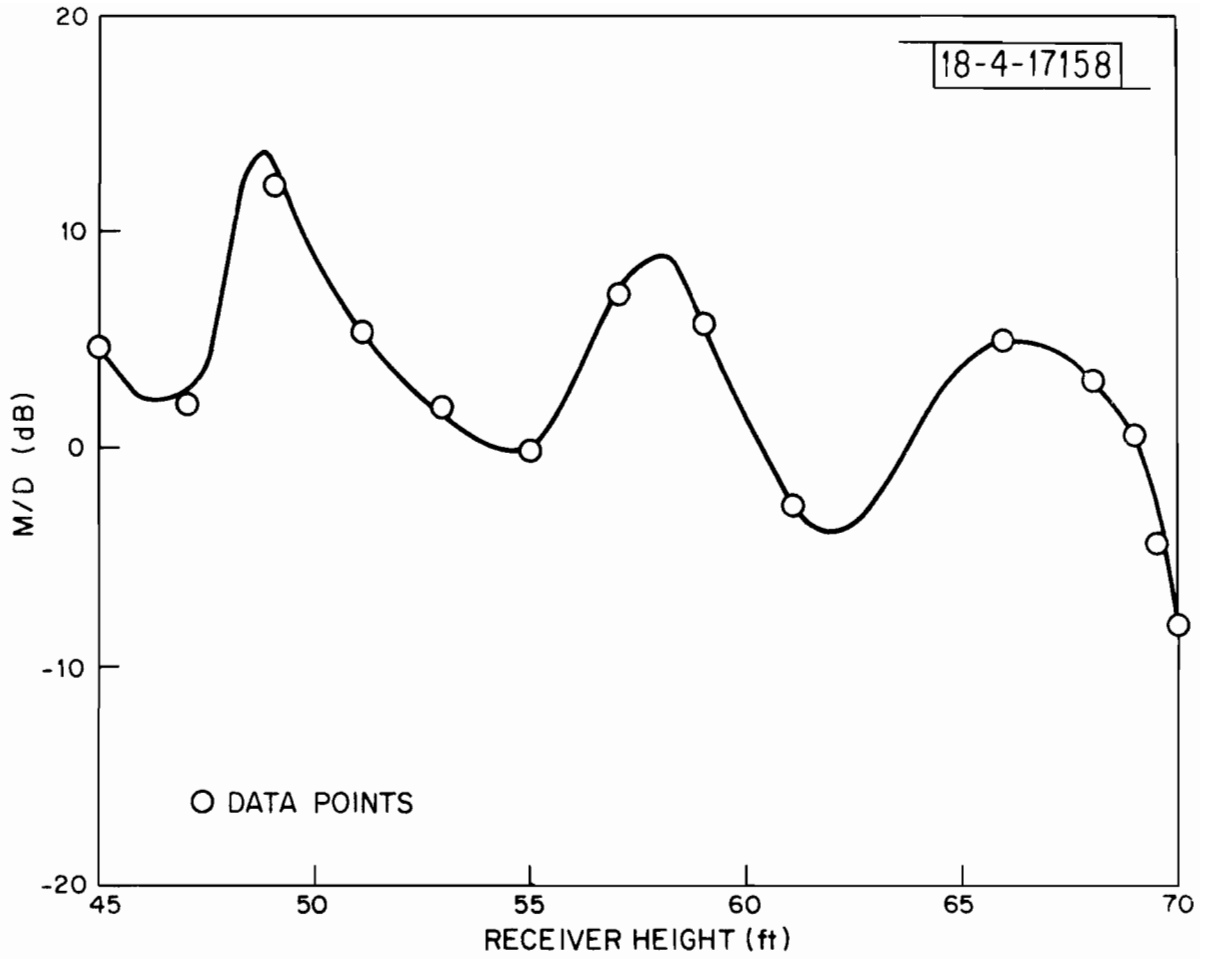


Fig. 14 Ground lobing for 11 December 1974 data.

## V. EXPERIMENTAL RESULTS

The data obtained from each experiment location are presented here. For convenience, we define the term,  $S_R$ , to be the surface area of the reflecting object associated with the first two or three Fresnel zones. This is the area that significantly influences the reflection level. For the data taken on or near the runways, the geometries and  $S_R$  were large. Since the terminal buildings were complicated and irregular over the areas,  $S_R$ , it was not surprising that multipath levels were, in general, low. The surface of hangars are often much more uniform and reflection levels potentially larger, but none were visible from the runways. The experiment was, therefore, moved to the North hangar area for the purpose of measuring reflections from the Delta hangar (building 21, Fig. 10). Because of space limitations, the geometries here were smaller. The smaller  $S_R$  and simpler building surfaces have the benefit of making it easier to use the data for model validation. Finally, reflection data from B747 and B727 airplanes were used to improve and verify the reflection model for airplanes.

The cw data used to monitor the experiment were recorded on strip charts and required no further processing. If only a single reflection is involved, then cw levels should concur with the pulsed data levels. Of course, there is no timing data from the cw, and if the pulsed data has not been processed, then we must rely on the unprocessed pulsed data for the determination that only a single reflection was involved.

### 5.1 Pier C Area Multipath

Figure 15 illustrates Pier C (building 33 in Figs. 10 and 11), which is located near runway 4L-22R. We note that the structure is a complicated one. The modeling issue is further compounded by numerous objects cluttered around it. If each of these objects causes significant direct or diffuse multipath, then the modeling problem would be almost impossible. However, unlike the monostatic radar where the desired signal is a weak reflection from an object, we are dealing with a bistatic case for which there is a strong direct signal from transmitter to receiver. All except the largest



Fig. 15 Pier C.

reflections should be small enough, compared to the direct, that they can be ignored (unless there is shadowing or cancellation of the direct signal). This argues that only large-scale objects, such as the building, need be considered for modeling. Such a hypothesis was under test in the experiments that were performed.

Three experiments associated with Pier C were performed. During the first experiment on 18 October 1974, the transmitter was positioned at the threshold end of runway 22L (position  $T_1$  in Fig. 11). For this and only this experiment, a horn was used for the transmitter antenna. The receiver, with its horn antenna at a height of 30 feet, traveled the length of runway 22L without a single reflection being observed on pulsed or cw data. Because the horn antenna was used, a large area was illuminated simultaneously. The cw was scalloped due to the combination of direct and ground bounce. A minimum detectable reflection was estimated to be about 30 dB below the direct level. This result is consistent with the stated hypothesis in that the main reflection from the building would occur, according to ray geometry, beyond the end of the runway. The transmitter was moved to a position ( $T_2$ , Fig. 11) down the runway on 24 October 1974 so that, according to ray geometry, reflections from Pier C should be observed at  $R_2'$  but not at  $R_2$  in Fig. 11. This geometry is reconstructed in Fig. 16 wherein distances and angles are shown. The transmitter was angled upward at  $1.6^\circ$  to control ground reflections and was rotated through approximately a  $70^\circ$  angle. At receiver position  $R_2$ , with an antenna height of 40 feet, there were no measured reflections at any angles. For position  $R_2'$  (same antenna height), the processed reflection data is shown in Fig. 17 and the levels, taking into account antenna patterns, are given in Table I. The angle associated with the peak reflection and the time differential between direct and reflected signals both concur with ray geometry reflections off Pier C. The peak level is -18.5 dB. We note that there are other reflections at an angle near  $59^\circ$ . By noting the time differential, the angle, and the position of  $T_2$  and  $R_2'$ , the

18-4-17159

24 OCT 1974

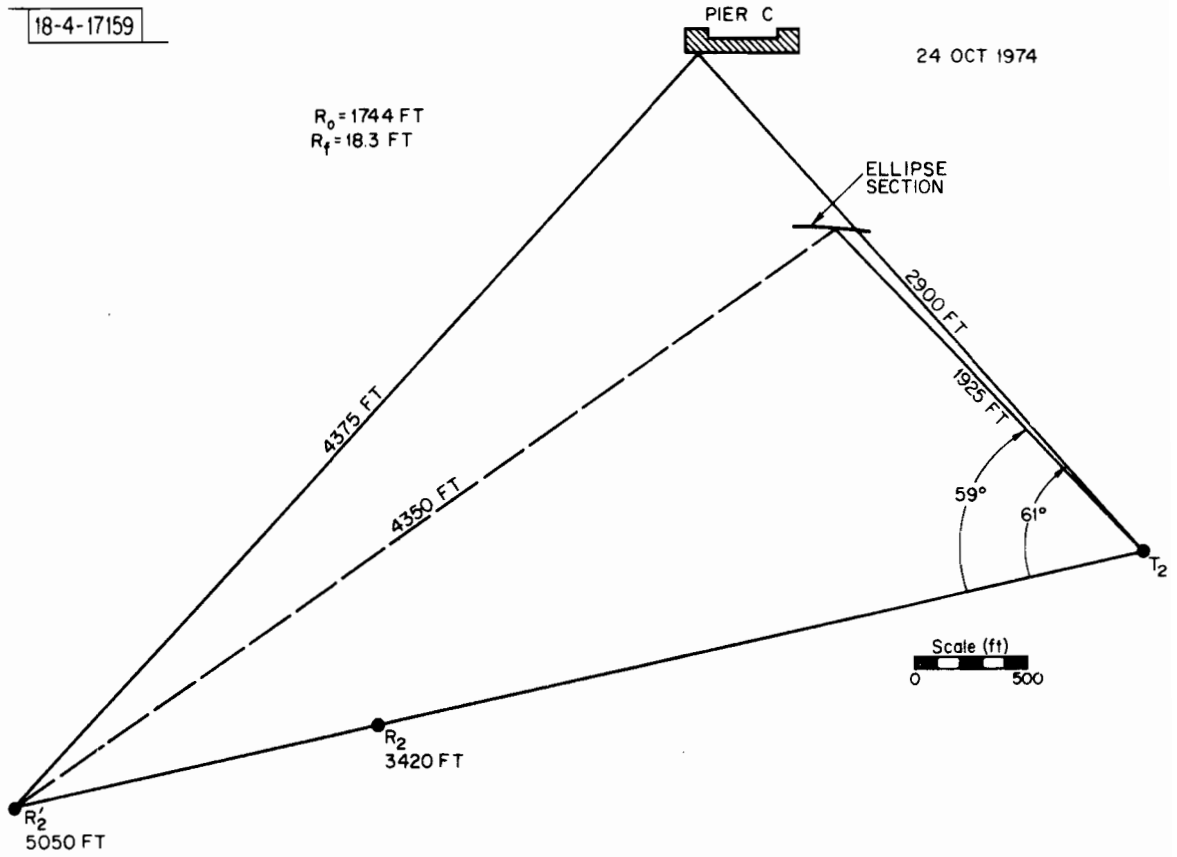


Fig. 16 Geometry for 24 October 1974.

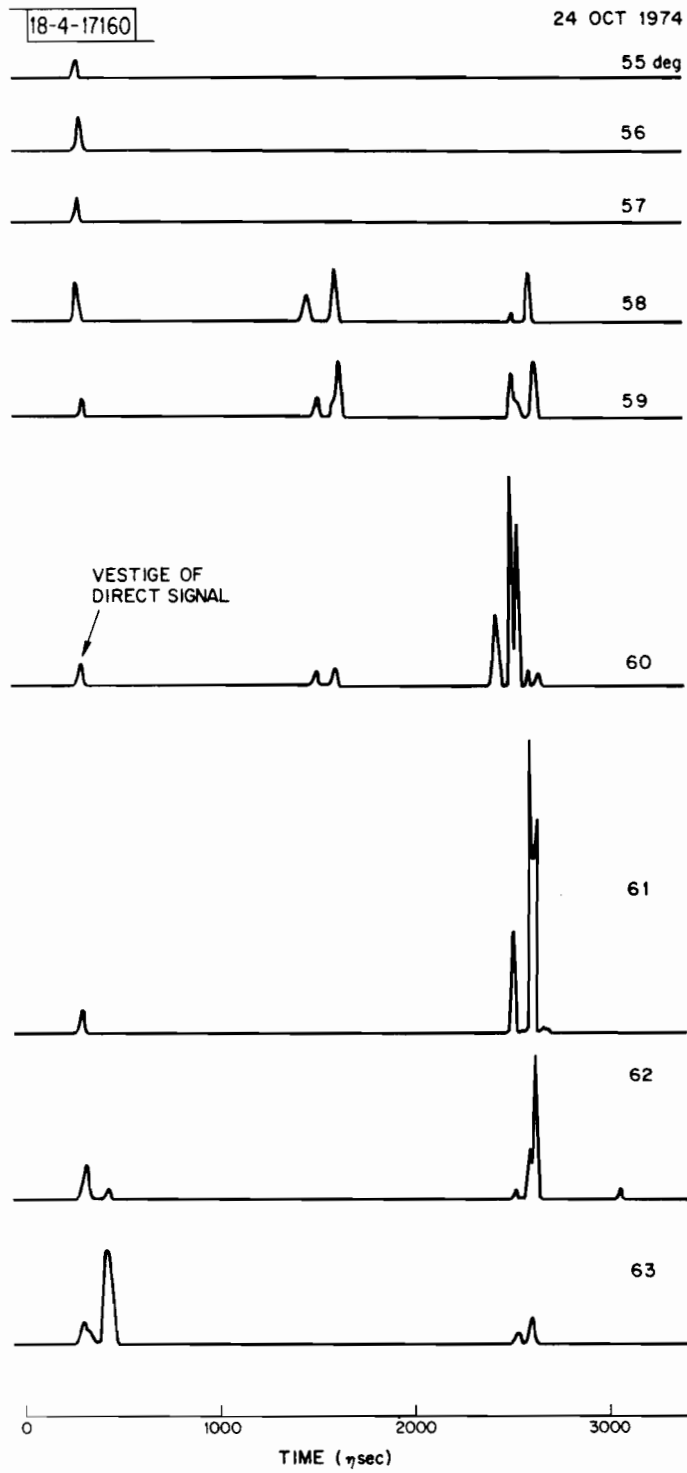


Fig. 17 Channel sounder processed output for 24 October 1974.

Table I

Transmitter at  $T_2$  Receiver at  $R_2'$ 

<u>Angle (deg)</u>	<u>First Reflection (dB)</u>	<u>Pier C Reflection (dB)</u>
55	---	---
56	---	---
57	---	---
58	-27.5	-27.5
59	-26.5	-25.5
60	-32.0	-20.0
61	---	-18.5
62	---	-21.5
63	---	-30.0

Time difference between direct and Pier C Reflection = 2300  $\eta$ sec (2250 feet).

Time difference between direct and 1st Reflection = 1250  $\eta$ sec (1225 feet).

reflecting object is located in taxiway F next to runway 4L-22R (on the Pier C side). We believe this was a plane on the taxiway waiting to cross 4L-22R.

The transmitter (with antenna tilted up at  $1.6^\circ$ ) was placed, on 9 December 1974, on runway 4L-22R (position  $T_3$ , Fig. 11) for the third position and two receiver locations  $R_3$  and  $R_3'$  were used. As shown in Fig. 18, specular reflections are expected at both receiver locations. At  $R_3$ , with the lower receiver antenna height set at 42 feet, the transmitter dish antenna was rotated and a peak determined at an angle  $59^\circ$  (see Fig. 18). A mast run was then performed and the results are presented in Table II. At some heights, there were two or three closely bunched reflections with average  $\tau_i = 800$  nsec. Table II and Fig. 19 show the largest of these. Figure 19 also shows the multipath model results. We see that, for this closer geometry,  $S_R$  is smaller and the peak reflection larger, as would be expected.

The receiver was moved 700 feet to location  $R_3'$ , and the direct signal should decrease by

$$\rho_R = \left( \frac{1850}{2550} \right) = -2.8 \text{ dB} .$$

The cw direct signal decreased by -3 dB. With antenna height again at 42 feet, an azimuth swing was performed and the peak level found at  $53^\circ$ . A height run was repeated and a few of the higher levels are:

42'	-23 dB
47'	-18 dB
49'	-17 dB
65'	-20 dB
70'	-19 dB
73'	-21 dB

so the levels dropped from peaks of -11 to -17 dB.

In the first experiment using the horn transmitter, a wide area was illuminated simultaneously without generating measurable reflections on the runway. For the second experiment on Pier C, an azimuth sweep through much

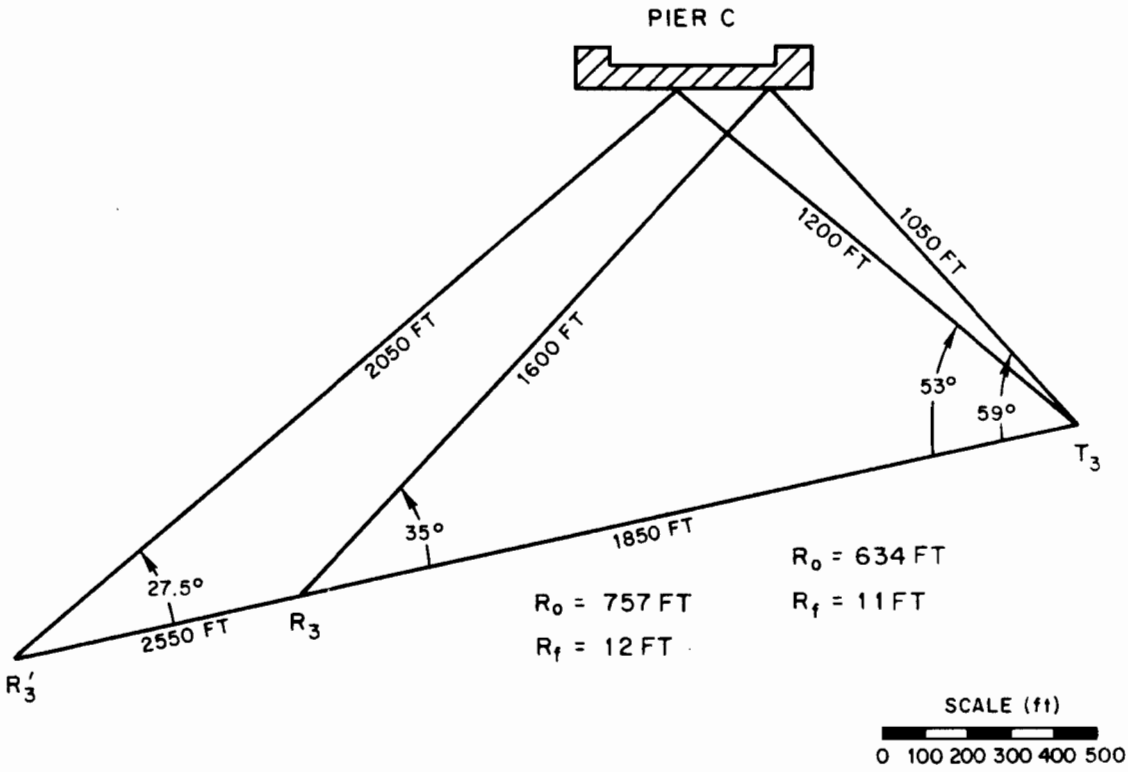


Fig. 18 Geometry for 9 December 1974.

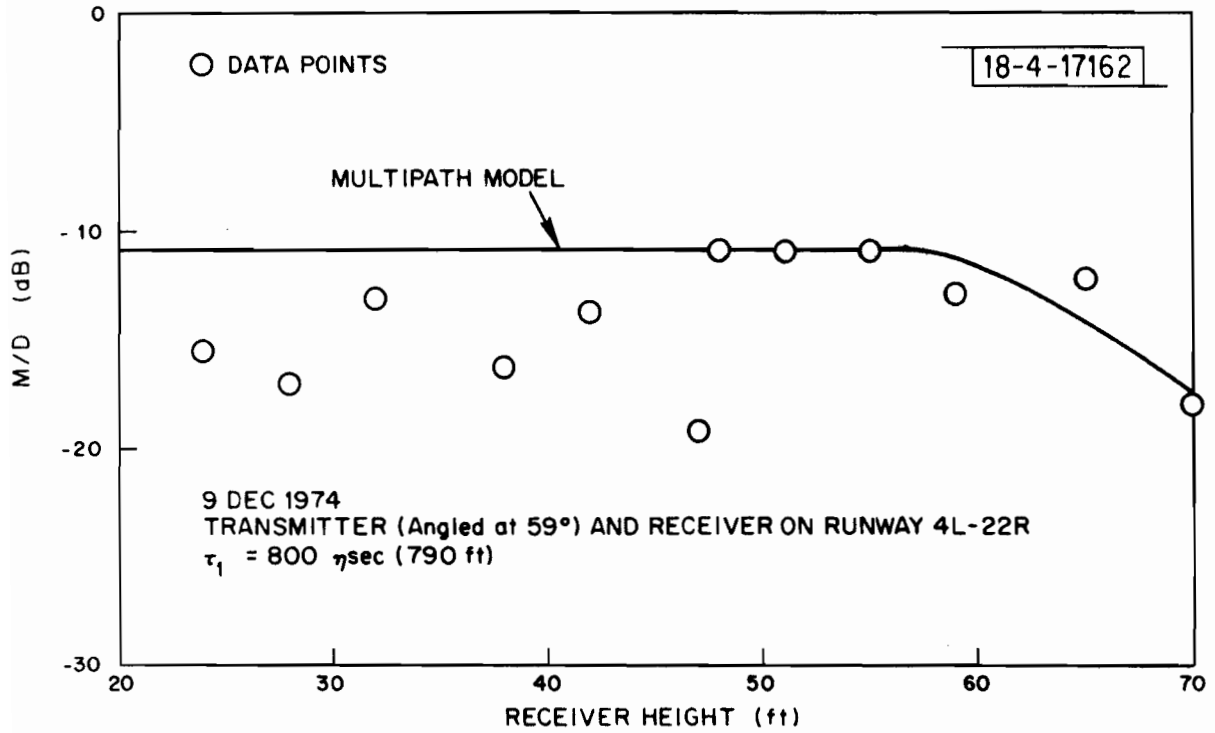


Fig. 19 Comparison of 9 December 1974 data with model M/D levels.

Table II  
Position R<sub>3</sub> With Transmitter Angled at 59°

<u>Receiver Antenna Height (ft)</u>	<u>Multiple Reflections</u>	<u>Peak M/D for Pulsed Data (dB)</u>	<u>cw Data (dB)</u>
24	No	-15	
28	No	-17	-13
32	No	-13	-11
38	Yes	-16.5	
42	Yes	-13.5	
47	Yes	-19	
48	No	-11	-13
51	No	-11	
55	No	-11	
61	Yes	-13	
65	Yes	-12	
70	Yes	-18	

$$\tau_1 = 800 \text{ nsec (790 feet)}$$

of the terminal area generated measurable reflections from only Pier C and the aircraft on taxiway F. This type of experiment was repeated for the third set of positions on 9 December 1974. Again, measurable reflection occurred when only Pier C was being illuminated directly. For the receiver location  $R_3'$ , the transmitter, angled for peak reflection, was left for 10 minutes and the levels remained constant except when the reflection path was blocked by a taxiing aircraft. All of these results support the hypothesis that this complicated building can be reasonably modeled by a flat plate with a suitable reflection coefficient.

### 5.2 Pier B Multipath

Pier B is a structure almost identical to Pier C; and on 25 October 1974 the transmitter was located at  $T_4$  and the receiver positioned for specular reflections off Pier B at  $R_4$ . This data has not been processed to yield M/D values. However, during the time the data was being taken, no reflections were noted except when the transmitter was aimed for specular reflections off Pier B. The levels of these reflections were very low (clearly lower than those measured on Pier C) which is what would be expected from the model for the geometry involved.

### 5.3 International Terminal Building

The International Terminal building, Fig. 20 (building 29 in Fig. 10), is located near the threshold of runway 33L. The glide slope for that runway is located just in front of the position  $T_5$  where our transmitter was located. The building is angled approximately  $14^\circ$  relative to the centerline of the runway and yields glide slope multipath at low scalloping frequencies in contrast to a Doppler Working Group study<sup>[8]</sup>, which has considered only buildings parallel to the runway. Possible EMI errors for time reference scanning beam and Doppler scan caused by this building are treated in Sussman and Orr<sup>[9]</sup>, which should be consulted for an in-depth discussion of the issues involved.



Fig. 20 The Volpe International Terminal.

Since a highly contentious issue in the U.S. MLS assessment (and possibly the ICAO AWOP assessment) was the immunity to inbeam E1 multipath from buildings near threshold, the reflection characteristics of this building were of particular interest.

Unfortunately, the data obtained on this building are incomplete on several counts. The equipment was not capable of measuring separation angle directly so it can only be estimated (see Sussman and Orr<sup>[9]</sup> for expected differences). Even with the extension pole the receiver antenna heights were limited to 70 feet so that we were unable to measure multipath at decision heights. Since the character of the building changes near the top (less cluttered and unbroken compared to lower portions, and it is tiered), reflections are expected to be much larger for geometries where the specular point is near the top\* (i.e., higher receiver locations). Finally, much of the pulsed data were not reduced in time to be included in this report.

Reflection data were taken on 23 October 1974, 11 December 1974, and 13 December 1974 with the transmitter position at T<sub>5</sub> and the numerous receiver positions indicated as I<sub>1</sub>, I<sub>2</sub>, ..., I<sub>7</sub> (see Fig. 11). The December pulsed data, which was far more extensive and included higher receiver positions than the October data, was not processed and we can present here only some cw results. The data are presented in Table III. Because of the transmitter proximity to the glide slope for runway 15R, the resulting reflections off the Volpe International Terminal (building 29, Figs. 10 and 11) correspond closely to actual multipath for the ILS. The building has a sheet metal covering. The transmitter and receiver locations are shown in greater detail in Fig. 21. Since we can assume, because of the 1.6° tilt in the transmitter antenna, that ground reflection can be ignored, then

$$M/D = \rho_R \rho_{RC} \rho_{FZ} \cdot$$

---

\*This suggests that a multipath measurement program using a portable TRSB ground equipment and a helicopter airborne receiver would provide a valuable supplement to help characterize building reflections.

Table III  
International Terminal

<u>Receiver Position</u>	<u>Transmitter Antenna Angle (deg)</u>	<u>Receiver Antenna Height (ft)</u>	<u>Multiple Reflections</u>	<u>Peak M/D (dB)</u>	
23 Oct 1974 (pulsed)	I <sub>2</sub>	40	22	No	-18
	I <sub>3</sub>	40	40	Yes	-17
	I <sub>4</sub>	38	40	Yes	-18
11 Dec 1974 (cw)	I <sub>1</sub>	33	22	No	-23
	I <sub>2</sub>	38	22	No	-12
	I <sub>2</sub>	38	40	No	-10
13 Dec 1974 (cw)	I <sub>3</sub>	38	22	?	-15
	I <sub>3</sub>	38	47	?	-10
	I <sub>7</sub>	38	39	?	-12
	I <sub>4</sub>	36	45	Yes	?

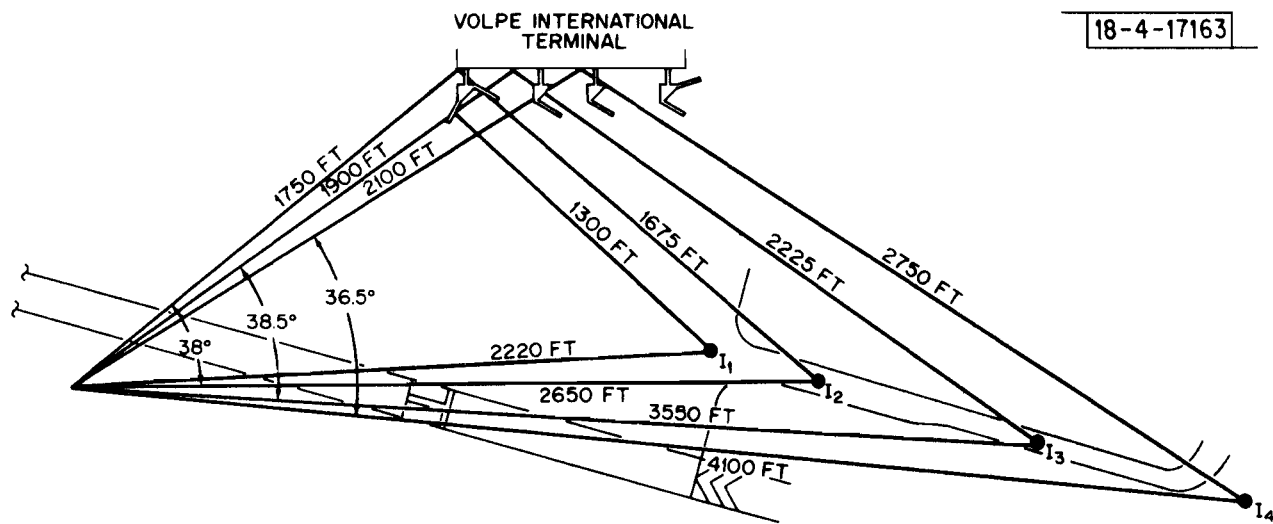


Fig. 21 Geometry for the International Terminal.

For receiver locations  $I_1$  to  $I_4$ , we have

$$-2.8 \text{ dB} \leq |\rho_R| \leq -1.5 \text{ dB} .$$

Although the building is metal clad and would have a  $\rho_{RC}$  of 1 for this construction material, we calculate, according to our model, an effective  $\rho_{RC}$  for the International building of

$$|\rho_{RC}| = -8.5 \text{ dB} .$$

Because the foregoing measurements correspond to a quite realistic geometry, we can estimate the multipath error that might be expected at runway 15R. In particular, we consider a TRSB EL1 system sited\* on the same side of the runway as the existing ILS glide slope. The peak reflection value from Table III is -10 dB. For a plane on a 20:1 glide slope at 150 feet above ground (see Fig. 22), the conical separation angle,  $\theta_m$ , would be

$$\begin{aligned} \theta_m &= \tan^{-1} \frac{140}{4000} - \tan^{-1} \frac{140}{2800} \\ &= 0.858^\circ \end{aligned}$$

and corresponds to a peak static error of

$$\epsilon_n = -0.118^\circ .$$

---

\* It is interesting to note some of the "real life" siting problems associated with an EL1 transmitter for runway 15R. Positioning it on the left side of 15R opposite the International Terminal, one has the problems imposed by terrain limitations and the perimeter road. Land fill could alleviate this situation but may be politically and legally unfeasible. Also, during the transition period between MLS and ILS, achieving coincident glide paths with a left side MLS site will be even more difficult due to the ILS critical area constraints.

On the other hand, siting the MLS EL1 on the same side of 15R as the International building could lead to reflection/blockage problems from wide bodied aircraft on the taxiways and parking apron.

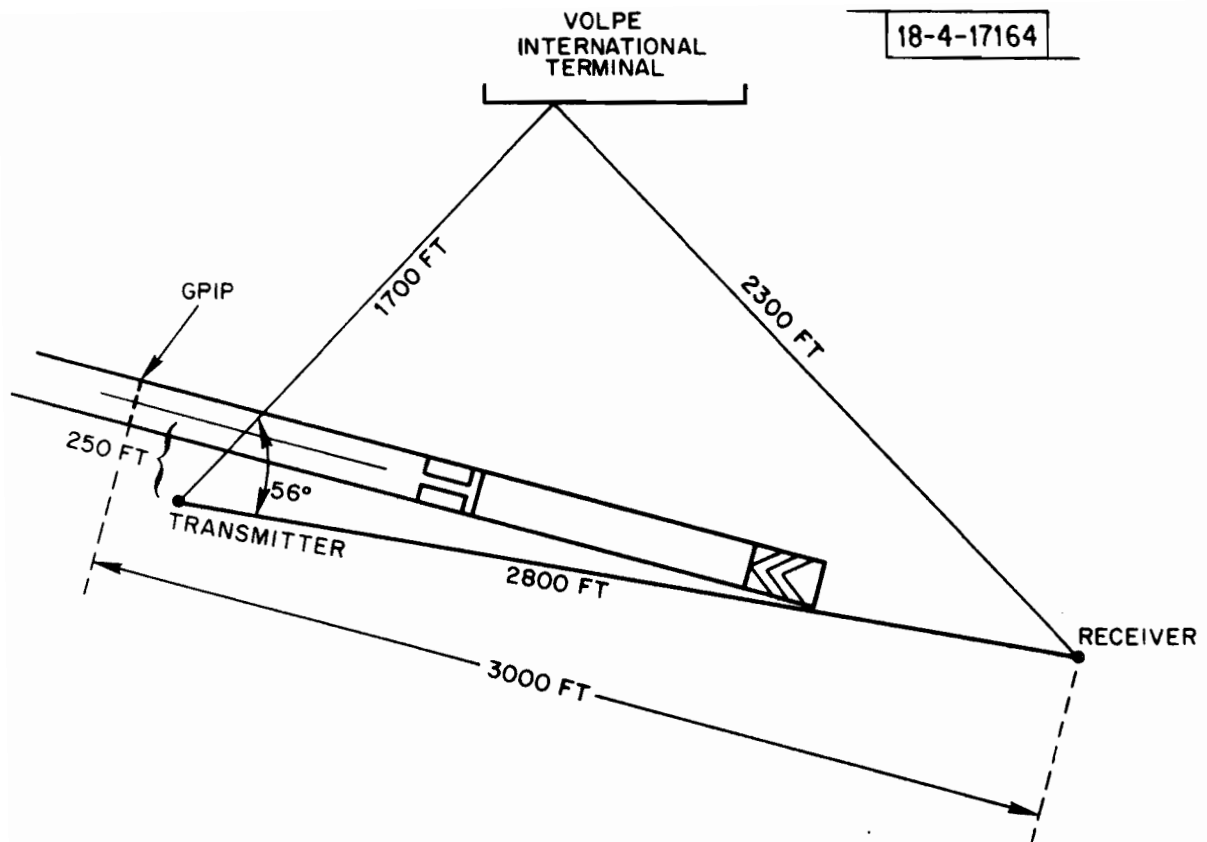


Fig. 22 Geometry for Runway 15R multipath from International Terminal.

The scalloping frequency for a plane approaching at 200 ft/sec is

$$f_s = 143 \text{ Hz}$$

which yields an averaging factor (determined in Ref. [9]) of approximately 1/4. The expected dynamic error would be about

$$\epsilon_n = -0.029^\circ \quad .$$

For a site location on the right side of 15R between the runway and a taxiway, the peak reflection from the International building would probably be 2 to 4 dB larger. This would be due to two factors: first, the path distance factor is 1 dB higher for this side, and second, the area  $S_R$  is smaller so that, for a complicated front such as this building, the peak measured level is likely to be 1 to 3 dB higher. The results for this site for an aircraft at a 176-foot altitude may be obtained in Table IV of Reference [9]. In there, for a conical separation in angle,  $\theta_m$ , of  $0.6^\circ$  and an M/D = -6 dB, peak static error is determined to be  $0.18^\circ$ , and scalloping frequency for the 200 ft/sec approach

$$f_s = 91 \text{ Hz} \quad .$$

The peak dynamic error is

$$\epsilon_n = 0.045^\circ .$$

These errors are large enough to be of concern but sufficiently small that they should not cause serious problems. The question remains, however, as to whether or not it is reasonable to extrapolate the levels of M/D measured at 40-foot receiver heights to the 150-foot altitudes.

In summary, this is an interesting case deserving attention. It may be representative of the type of problems MLS operation is likely to encounter; a large metal clad building near threshold, significant restriction on EL1 siting, and the building angled relative to the runway centerlines. The data is incomplete mainly due to equipment deficiencies. The unprocessed December pulsed data would yield some reflection values at heights of 70 feet,

but it would be far more interesting to measure M/D ratios between 100 to 200 feet.

#### 5.4 Delta Hangar

It is fairly common to discover that hangars are visible from airport runways, although this is not the case at Logan. We, therefore, moved to the North hangar area to measure reflections off of the Delta hangar. The building (no. 21 in Figs. 10 and 11) is shown pictured in Fig. 23.\*

In the experiments performed in the North hangar area, the dimensions of the measurement geometries were constrained by physical structures to be smaller than that expected in a "realistic" airport configuration. This situation results in the surface area  $S_R$ , defined earlier, being smaller than in the previous cases. This fact coupled with the relative simplicity of the hangar leads us to expect that, for some geometries, the hangar surface is likely to be homogeneous over  $S_R$  or a large part of  $S_R$ . The resulting measurements would be used primarily for validation of the computer multipath model.

The transmitter position,  $T_G$ , is shown in Fig. 11 as are receiver locations  $R_G$ ,  $R_G'$ , and  $R_G''$ . These have been translated onto graph paper in Fig. 24. For receiver location  $R_G$ , the cw reflection peaks at an angle of  $-33^\circ$  at the level of  $M/D = 8.5$  dB. The receiver antenna is at a height of 22 feet. The specular point on the building is near the juncture of the cinder blocks and the fiberglass windows on the hangar doors. No measurable reflections were observed off the fiberglass so we can assume  $\rho_{RC} \approx 0$ . For the cinder block, we expect  $\rho_{RC} \approx 0.8$ .

The geometry here is such that the ground reflection terms are negligible, in which case the multipath model yields

---

\* Hangar buildings seem to be far simpler structures than terminal buildings. This determination is made from direct observation at airports and from a survey of airport buildings done at several major airports (JFK, PHL, SFO, LAX, ORD, MIA, TUL, MSP). This implies that many should be successfully modeled by one or two plates for which the reflection coefficients may be ascertained from the known construction materials.



Fig. 23 The Delta hangar.

8 DEC 1974 AE 4-17156

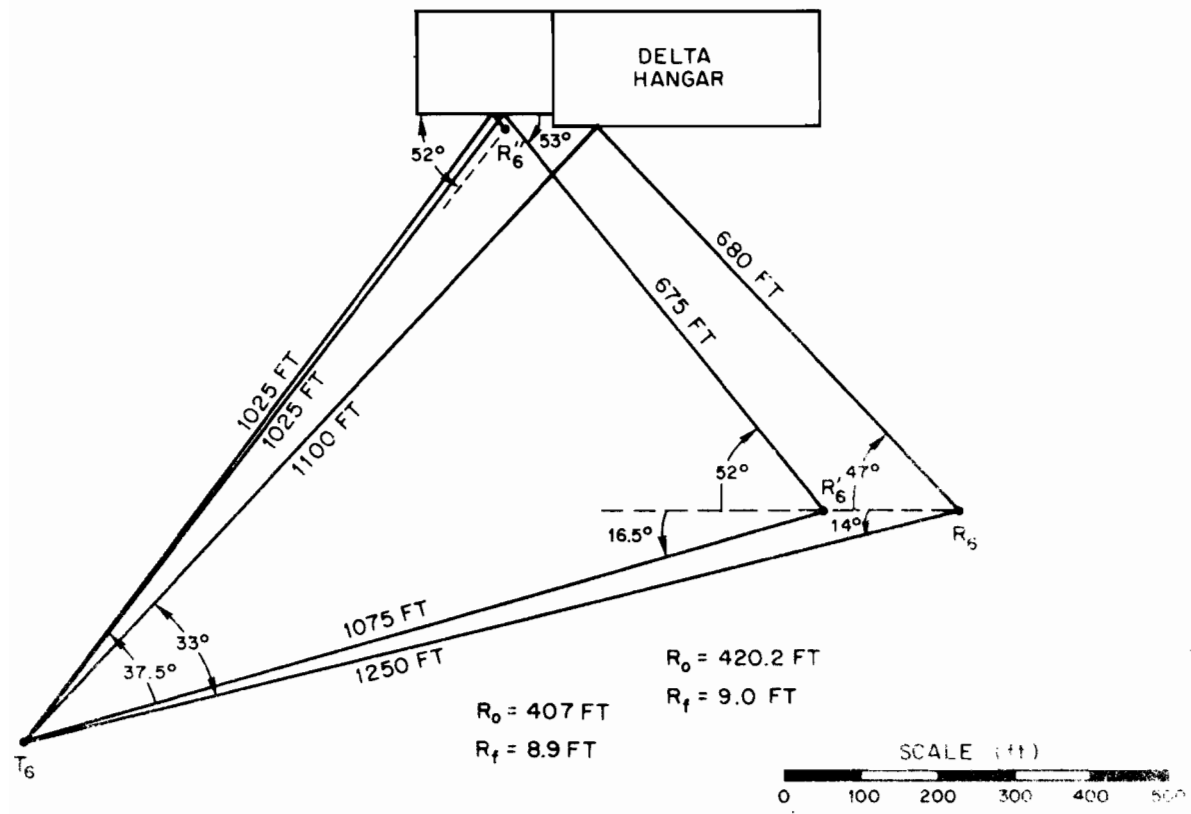


Fig. 24 Geometry for 8 December 1974.

$$M/D = \rho_R \cdot \rho_{RC} \rho_{FZ} \approx -7 \text{ to } -10 \text{ dB}$$

where  $|\rho_R|$  = path distance factor  $\approx -3$  dB

$|\rho_{RC}|$  = Fresnel reflection coefficient  $\approx -2$  dB

$|\rho_{FZ}|$  = factor for width of cinder blocks  $\approx -2$  to  $-5$  dB, depending on specular point location

The cw measured value was  $-7$  dB in this region which agrees well with the model.

At receiver position  $R_6'$ , there is but a single reflection so cw and pulsed data should agree. Figure 25 shows a plot of the M/D ratios vs. the antenna height for each. The curves agree in shape but there is a 10 dB discrepancy between them. The cw data appears to be at the correct level since it was more reliably obtained and is consistent with other data. For the pulsed data, a questionable value from the horn antenna pattern was used (the  $90^\circ$  value of the azimuth pattern) and the possibility of an unaccounted 10-dB pad exists. (Note that, since the upper horn antenna used for pulsed data is angled  $30^\circ$  relative to the lower antenna, the questionable  $90^\circ$  pattern value is not used for that data.) Figure 25 and Table IV show, at the higher heights, some large M/D ratios. The Delta hangar consists of two adjacent buildings (a metal clad building on the left and a cinder block and fiberglass building on the right). For receiver position  $R_6$ , the reflection was off the building on the right. For locations  $R_6'$  and  $R_6''$ , the reflections are off the building on the left. At a receiver height near 70 feet, the specular point is at about a 42-foot height which places it approximately in the middle of the metal upper section (it extends from 30 feet to 50 feet at the peak). The model predicts (with  $\rho_{RC} = 0$  dB and  $\rho_{FZ} \approx -1$  dB,  $\rho_R = -4$  dB)

$$M/D = -5 \text{ dB}$$

as compared to a measured level of  $-4.5$  dB. As the antenna is lowered, the specular point approaches the edge of the metal section. We can compare this data with the multipath model. This is done in Fig. 26 where we see there is good agreement between them.

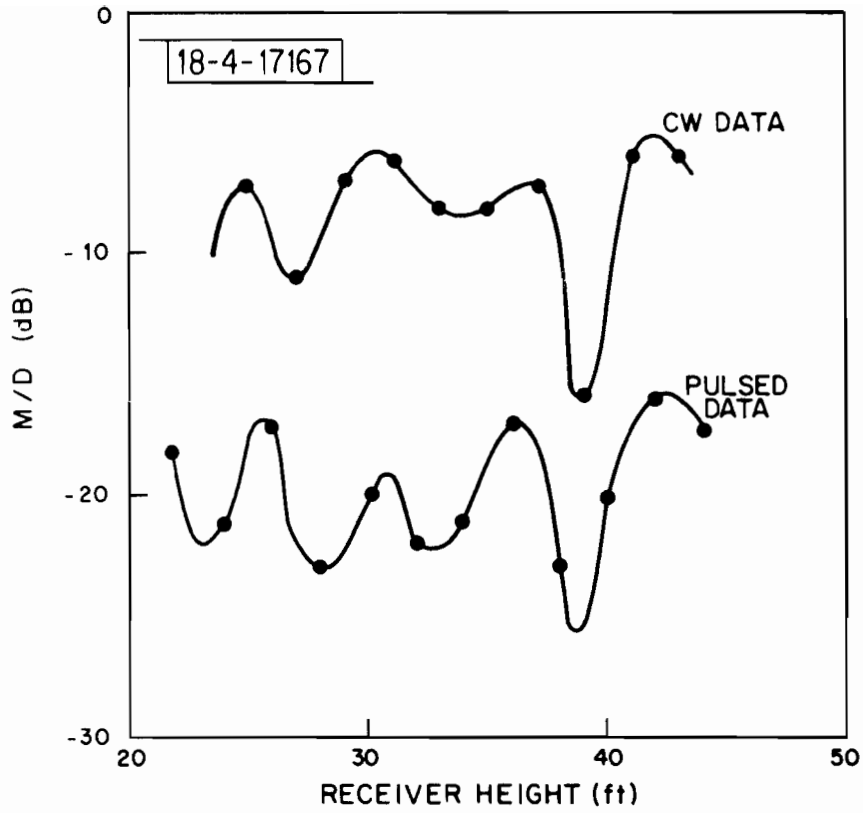


Fig. 25 Comparison of lower antenna pulsed data and cw data.

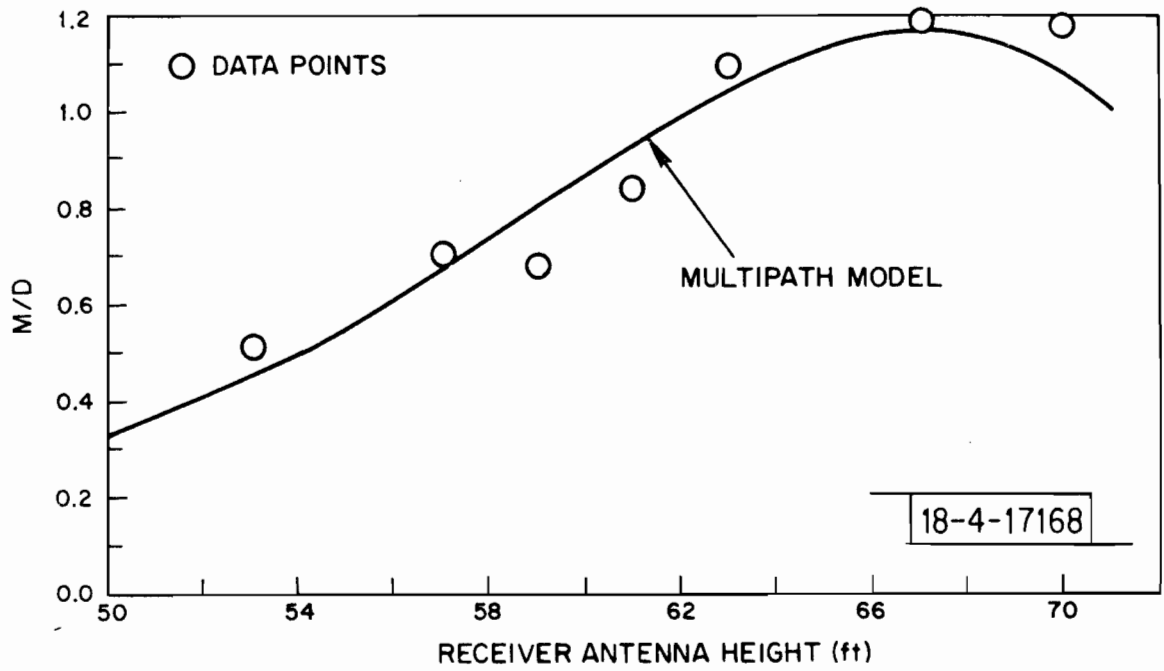


Fig. 26 Comparison of 8 December 1974 data with multipath model M/D results.

Table IV  
 Transmitter at T<sub>6</sub>, Receiver at R<sub>6</sub>'

Receiver Antenna Height (feet)	M/D (dB)
53	-14
55	- 8
57	-10
59	-11
61	- 8
63	- 5
65	- 6
67	- 4
70	- 4.5

$$\rho_R = \frac{1075}{1700} = 0.63 \text{ (-4 dB)}$$

Angle of Transmitter Antenna = -37.5°

Table V

Transmitter at  $T_6$ , Receiver at  $R_6''$

<u>Antenna Angle (deg)</u>	<u>22-foot M/D (dB)</u>	<u>45-foot M/D (dB)</u>
-7	-15	-20
-6	- 8	-12
-5	-10	-20
-4	- 6	- 6
-3	- 5	0
-2	- 5	0
-1	- 7	- 2

Receiver Antenna Heights = 22 feet and 45 feet

Data taken at receiver location  $R_6''$  (Table V) were obtained specifically for model verification. For the upper antenna at a height of 45 feet, we expect the observed M/D = 0 dB and for the lower antenna at 22 feet, the measured M/D = -5 dB can be used to compare to that  $R_6'$  data for which the specular point was at 22 feet. This corresponded to a  $R_6'$  receiver height of 36 feet. The model prediction yields ( $\rho_R = -4$  dB,  $\rho_{RC} = -5$  dB)

$$M/D = -9 \text{ dB}$$

compared to the measured value of approximately -7 dB. Considering the fact that the building is not of a homogeneous material, this is a reasonably good agreement.

The values realized in the experiment have been well represented by those generated by the model. It is, therefore, reasonable to extrapolate model results to geometries for which data was not obtained. The implication of this is that if such a hangar were located near the threshold of a runway, as is the International Terminal, then one could expect it to yield significant levels of multipath.

### 5.5 NAFEC Data

There was a modicum of data taken at NAFEC where the equipment was first assembled. These data were taken primarily to test the equipment and only one section of the data, taken on 7 October 1974, was processed. On 8 October 1974, some screen data was taken but, the antenna was not properly tilted to avoid ground reflections and the data was corrupted by ground reflections.

The section of processed data was of reflections from the rear of hangar building 301 pictured in Fig. 27. The geometry is shown in Fig. 28 where the transmitter location and receiver paths are designated. The terrain is sloping down from the building so that the ground level at the transmitter was about 15 to 20 feet below the ground level at the building. The ground at the receiver is also lower by about 10 to 15 feet. The receiver antenna height was 45 feet and the transmitter 10 feet above their respective ground heights. The transmitter antenna is aimed directly at the corner of the building.

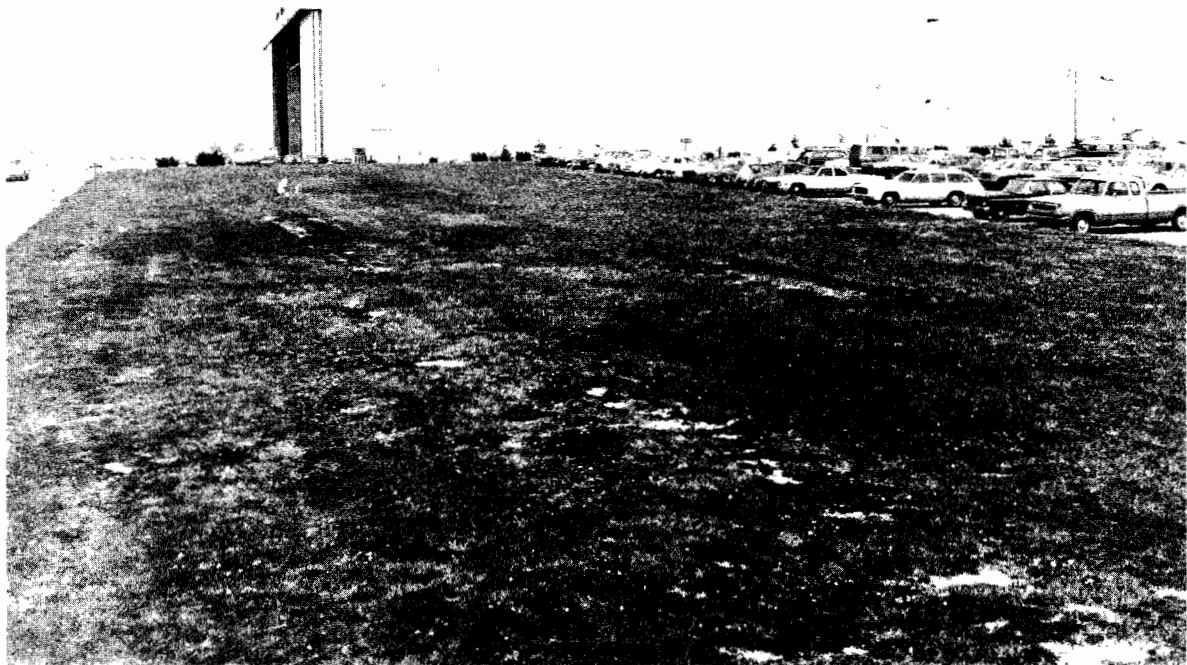


Fig. 27 Rear of NAFEC hangar building no. 301.

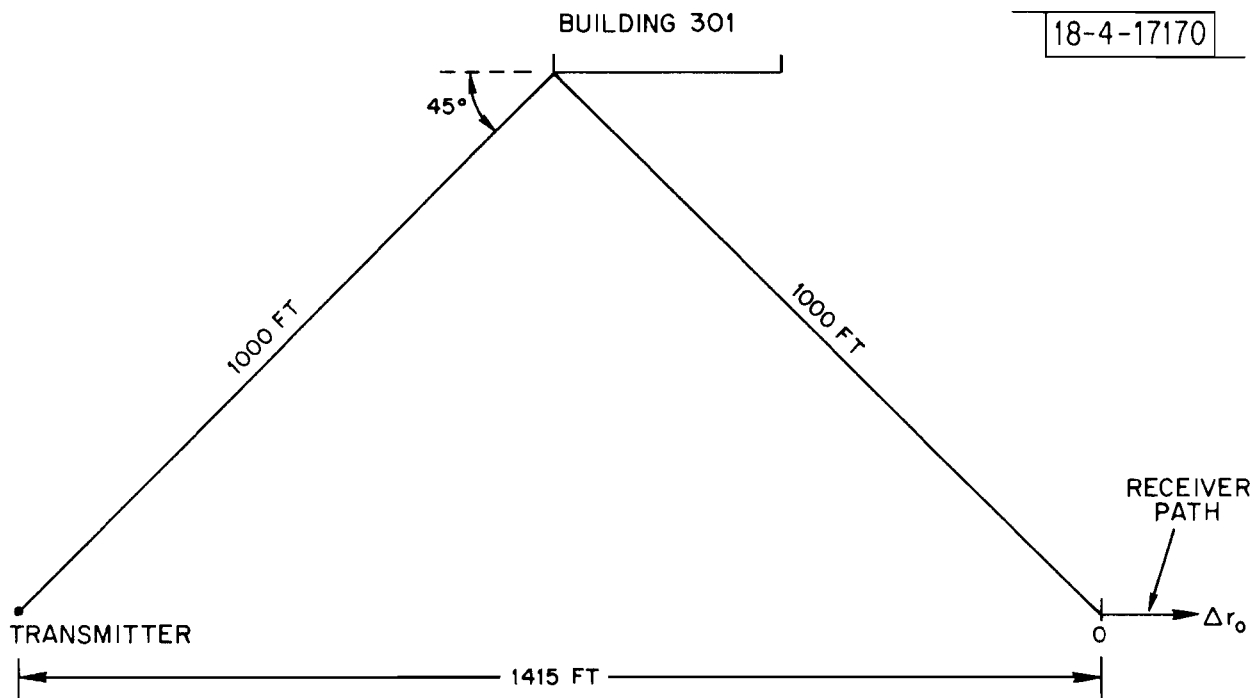


Fig. 28 Geometry for NAFEC, 7 October 1974.

Figure 29(c) indicates the approximate receiver output curve, as a function of receiver position  $\Delta r_0$  (as defined in Fig. 28), to be double peaked. The expected curve for a smooth, unbroken wall is shown in Fig. 29(b) where the effect of the dish antenna pattern is included (Fig. 29(a)). The measured M/D levels are corrupted by ground reflections, but these should not influence the shape of the curve over the relatively short range of the receiver path. This can be seen by considering the change in direct path,  $\Delta r_0$ , between adjacent ground reflection peaks.  $\Delta r_0$  satisfies the equation

$$\frac{2H h}{\lambda(r_0 - \Delta r_0)} - \frac{2H h}{\lambda r_0} = 1$$

$$\Delta r_0 = \frac{\lambda r_0^2}{2H h} \approx 2600 \text{ feet.}$$

where  $h$  and  $H$  are the transmitter and receiver heights, respectively. By contrast, the  $\Delta r_0$  for the receiver path was less than 200 feet, which suggests that another mechanism causes the double peaked behavior.

We note in the picture of the hangar buildings that there is an 11.5 feet x 15 feet recessed metal door about 23 feet from the edge. If the specular point is, as estimated for the direct reflection, at the 14- or 15-foot height, then a portion of the door would be in the first Fresnel zone for  $\Delta r_0$  between 45 to 70 feet. The multipath model curves for a reflection from the cement wall ( $\rho_{RC} = 0.4$ ) with the door size opening and for the metal door ( $\rho_{RC} = 1.0$ ) by itself are shown in Fig. 29(d). The effect of the antenna pattern is included in these graphs. The relative phases of these two curves is unknown, thus rendering correctly phased additions impossible, but it is certainly possible that some combination of these two curves could produce a result similar to Fig. 29(c).

## 5.6 Airplane Multipath

The model used for aircraft reflections is comprised of a cylinder for the fuselage and sections of two cylinders mounted back to back for the tail<sup>[1]</sup>. This model had not been compared to field data to any real degree and,

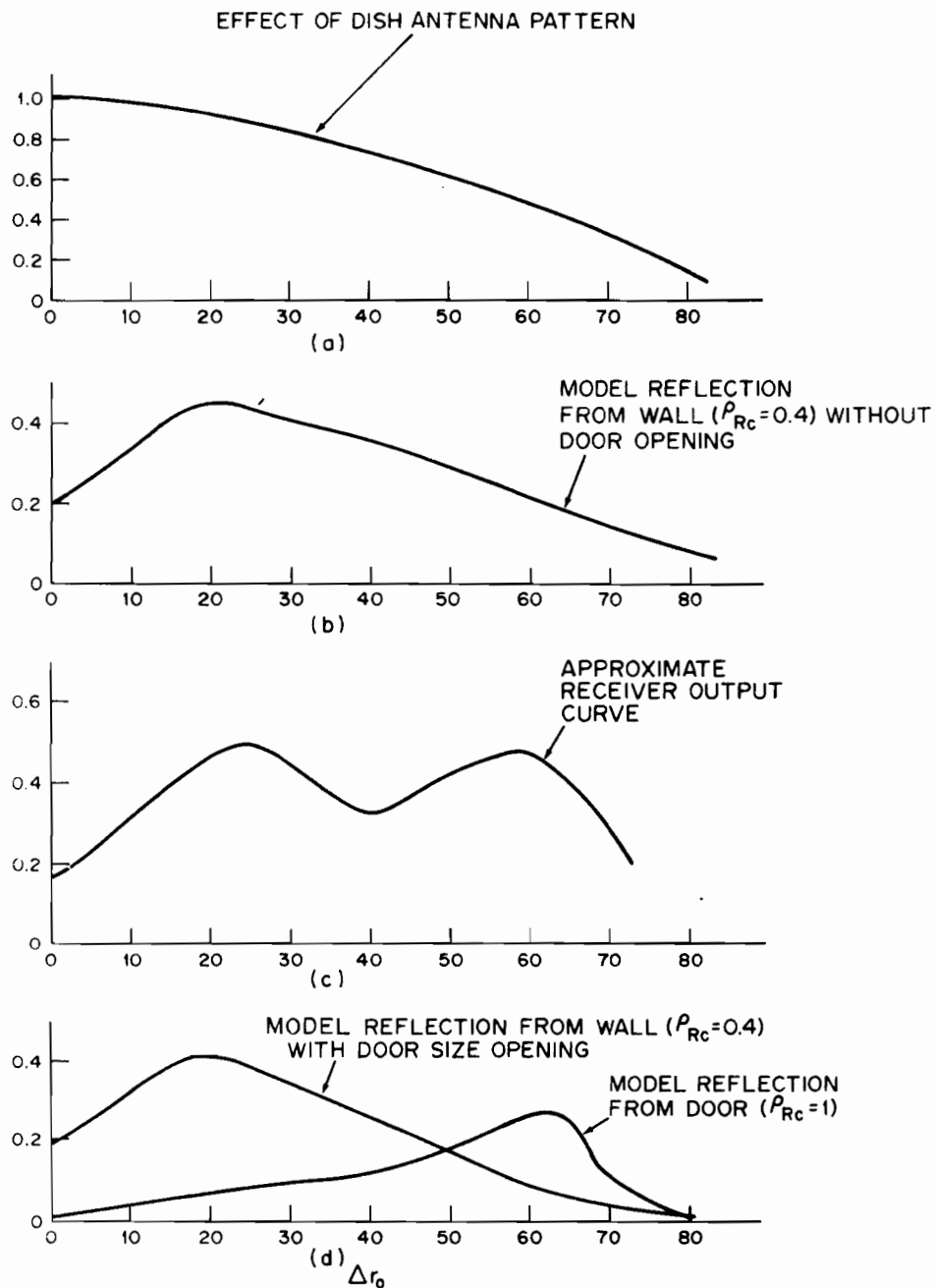


Fig. 29 Comparison of 7 October 1974 data with multipath model M/D results.

consequently, the multipath measurements for airplanes performed the dual roles of helping to choose improved parameter values as well as verifying the model.

Each experiment on the aircraft generated large reflections from the tail and small ones from the fuselage due to the fact that the front and rear of the fuselage are double curved and the wing caused blockage in the center. It was found that there was better agreement between the measurement and model by using the largest tail fin length rather than the average. This increased the extent but not the level of the reflection. It was also found that exaggerating the tail height was desirable to increase the vertical extent of the model reflection.

#### 5.6.1 Boeing 747 Airplane

Multipath data for Boeing 747s were obtained on four occasions, but one set was corrupted by ground reflection and for a second, only cw data was obtained. The two remaining sets were taken on 11 and 12 December 1974. The transmitter and receiver locations for each are shown in Fig. 30, denoted by subscripts 11 and 12, respectively. The latter set of data is presented first because it is more extensive. The geometry is shown in more detail in Fig. 31. Note that the angle of the incoming ray relative to the airplane axis is  $20^\circ$ , while the outgoing ray is  $35^\circ$ . The curvature in the tail is responsible for this result. This geometry, coupled with the fact that the transmitter antenna has only a  $2^\circ$  beamwidth, eliminates the possibility of a fuselage reflection so that we can compare the data directly with the tail reflections of the model. The transmitter antenna was angled up at  $1.6^\circ$  to control ground reflections so they can be ignored. An azimuth swing was performed at receiver position R and found to peak at  $11^\circ$  at a level of -8 dB. The receiver was moved on a radial to R', and first an azimuth swing was done followed by a mast run with the transmitter fixed at an  $11^\circ$  angle. For the azimuth swing we obtained two reflections separated by about 55 nsec. The first is probably due to reflections of an engine pod; the timing and angle are consistent with this interpretation. The peak of this first reflection is at a level of -19 dB and occurs at  $10^\circ$ . These reflections have not been included in the model since

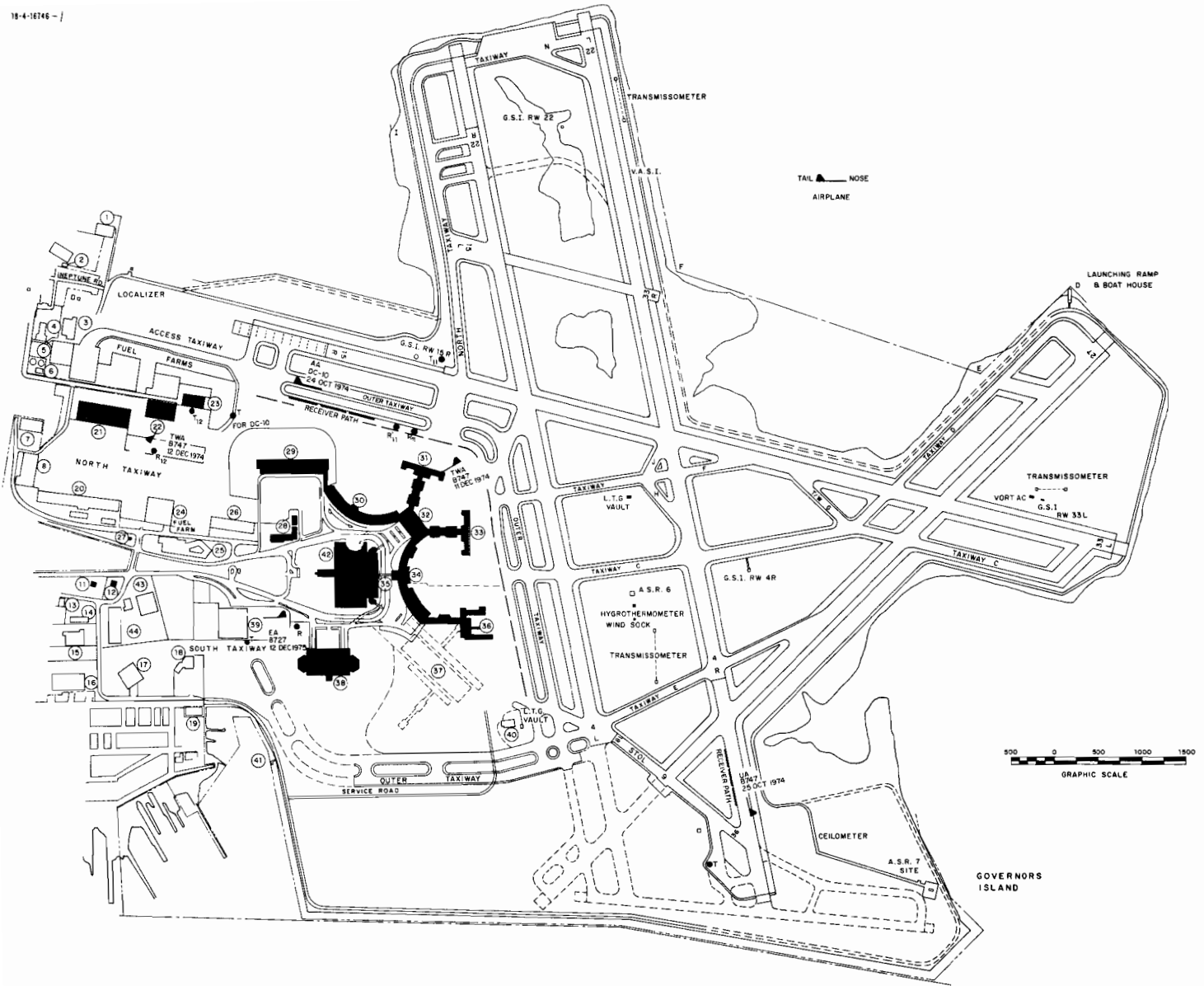


Fig. 30 Location of aircraft, transmitters, and receivers for airplane multipath experiments.

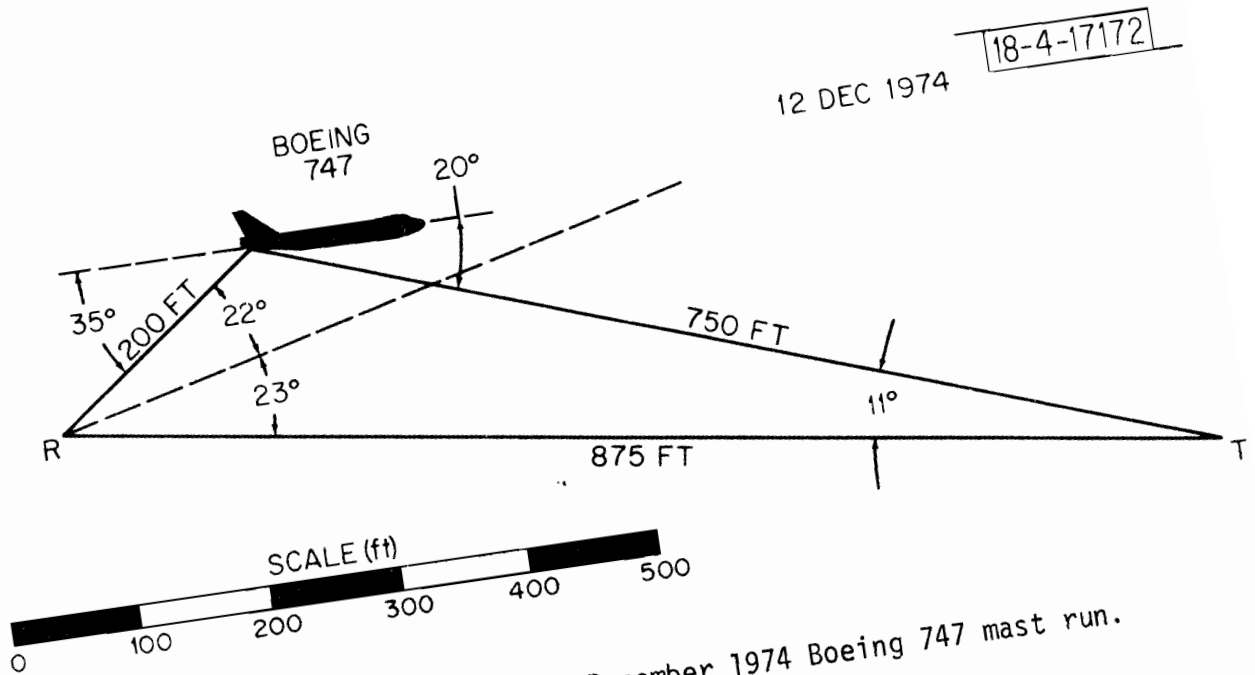


Fig. 31 Geometry for 12 December 1974 Boeing 747 mast run.

engine pods have been ignored. This peak level is small enough compared to the tail peak that it can reasonably be ignored. The most data run are shown in Table VI. The dimensions were small and it was necessary to estimate the vertical antenna pattern and use it in determining Table VI. A comparison of the model M/D values, after the suggested parameter modifications vs. the data, is shown in Fig. 32. It should be mentioned that changes in these parameters did not affect levels but only the angles and extent over which reflections were observed.

A comparison of the R and R' data can be done by reference to the equation of Riblet and Barker<sup>[6]</sup> in which the reflection from a cylinder oriented as is the tail is given by

$$\rho = \sqrt{\frac{1}{1 + \frac{2R_0}{R_c} \sin \alpha}}$$

where  $R_c$  is the radius of the cylinder and  $\alpha$  is the angle of incidence. Using

$$\alpha = \frac{20^\circ + 35^\circ}{2} = 27.5^\circ$$

and

$$R_c = 80 \text{ feet}$$

then we have

$$\rho = \sqrt{\frac{1}{1 + 0.05414 R_0}}$$

For location R,  $R_0$  is 88.24 feet; and for R',  $R_0$  is 157.9 feet, so that at R

$$\rho_R = 0.42 \text{ (-7.6 dB)}$$

and at R'

$$\rho_{R'} = 0.32 \text{ (-9.8 dB)}$$

We therefore expect a 2.2-dB difference between the R and R' levels at 44 feet. The data yielded -8 dB at R and -11 dB at R', a 3-dB difference.

Table VI

B747 Multipath Data, 12 December 1974

<u>Receiver Antenna Height (ft)</u>	<u>M/D (dB)</u>
16	-26
18	-24
20	-25
22	-32
24	-23
26	-23
28	-28
30	-26
32	-27
34	-18
36	-12
55	- 7
57	-19
59	- 6
61	-14
63	- 7
65	- 8
67	- 3
69	- 8

Looking at Fig. 32, we note that M/D falls off at about 35 feet corresponding to a specular point height of about 28 feet, just about the height of the horizontal stabilizer (Fig. 33). This could be due to one or more of the following: shadowing from the wings, scattering from the horizontal stabilizer, and the specular point lying off the plane (the bottom of the plane at the tail end is about 20 feet high).

The geometry for the 11 December 1974 data is presented in Fig. 34. The grazing angle is about  $68^\circ$ ; so that the transmitter and receiver are near broadside of the aircraft and there are both tail and fuselage reflections being received simultaneously. The transmitter is on lower terrain than the airplane, and ground reflections are likely to be included in the received signal. The peak fuselage model M/D and the tail M/D levels are shown in Fig. 35. Also shown are the sum and difference of these two reflections together with the data points. There is an anomalous peak of -6 dB near the 24-foot antenna height corresponding to a specular height of 20 feet at the plane. This corresponds to the height of the lower corner formed by the horizontal stabilizer and the fuselage. Since  $R_f$  is about 10 feet and the horizontal stabilizer is about 20 feet, we conjecture that this peak is due to the focusing effect of this corner. The model is deficient in picking up this peak, but it appears that a peak such as this would occur over only a small range of transmitter and receiver geometries since it did not appear in any other experiment.

In each geometry, the tail reflections dominated the data in that they were, in general, as large or larger than the fuselage reflection and they occurred over much larger angles. The reflections generated by the model agree well in extent and level, with the singular exception of the anomalous peak.

#### 5.6.2 Boeing 727 Airplane

The Boeing 727 (Fig. 36) is one of the most common planes found at major airports. It and the L1011 are somewhat unique in that an engine, located at the base of the tail, is molded smoothly onto the tail and the fuselage to form a relatively large, flat area on the airplane. On the evening of 12 December

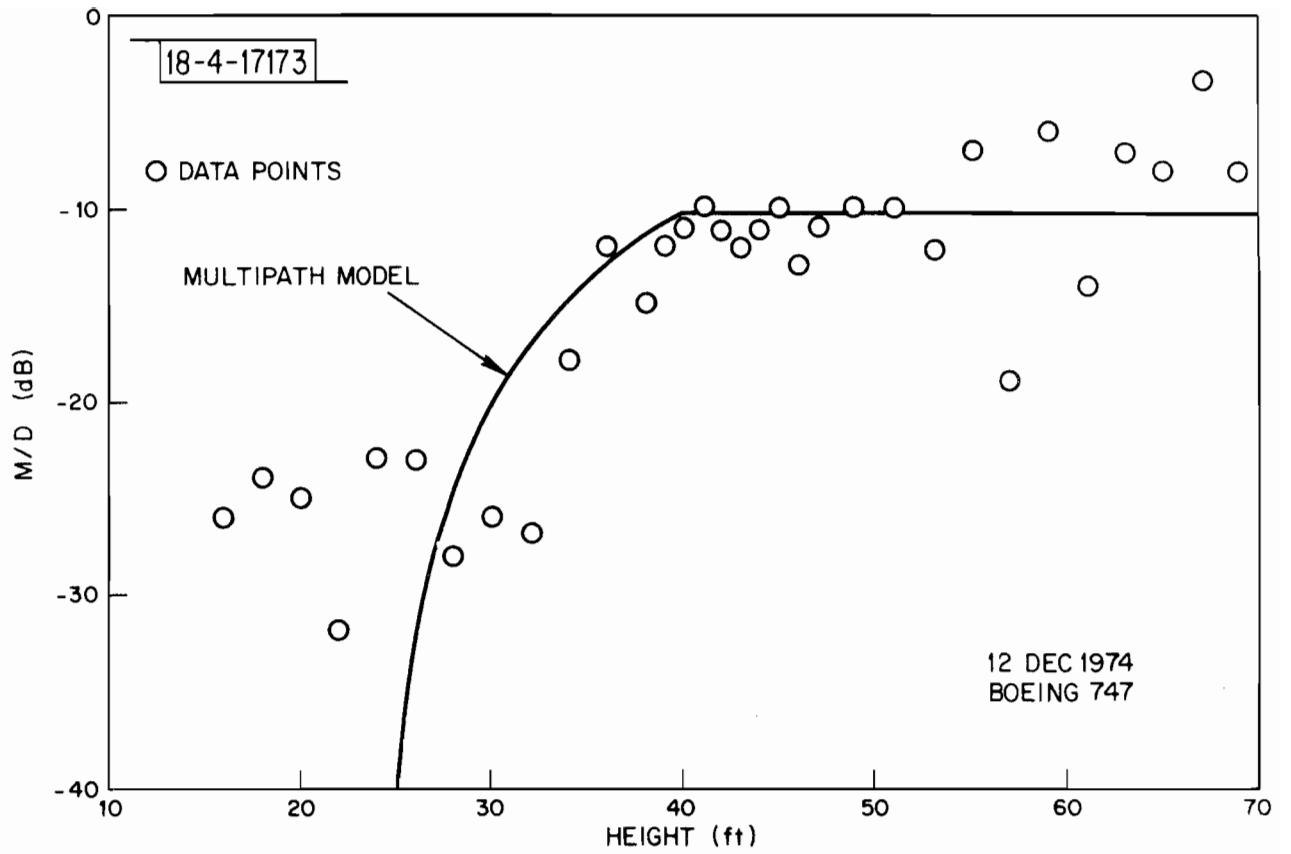


Fig. 32 Comparison of 12 December 1974 data with multipath M/D results.

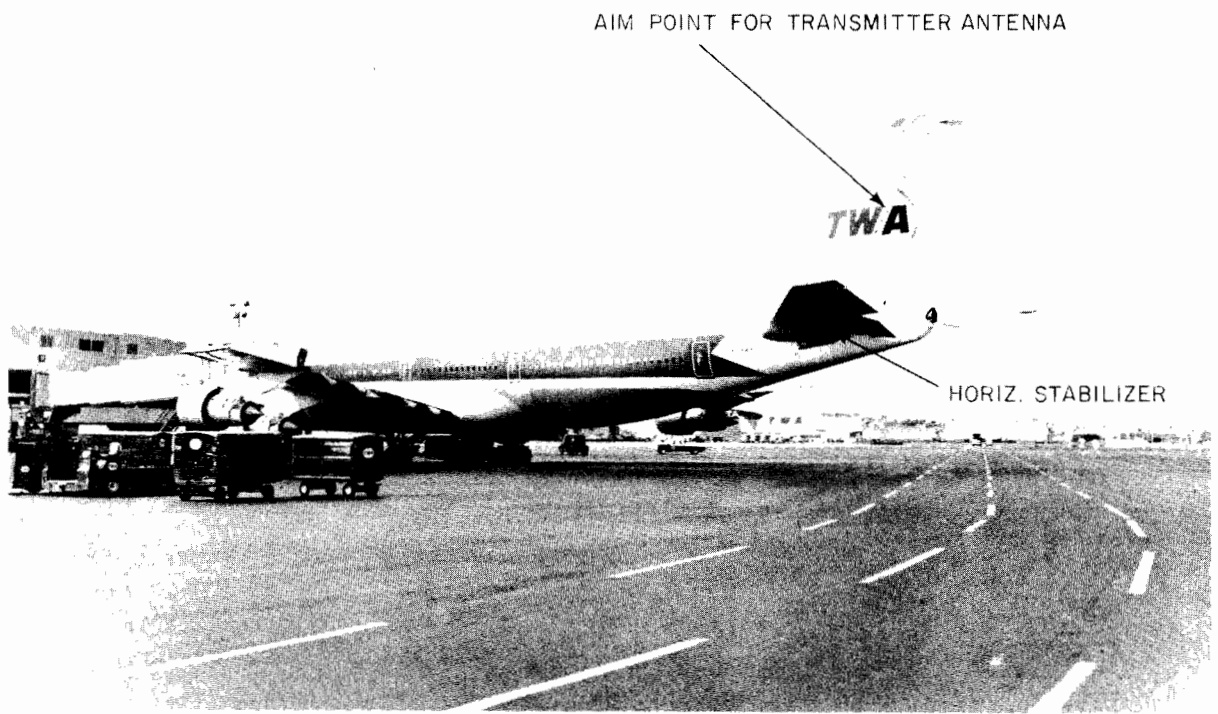


Fig. 33 Boeing 747 airplane.

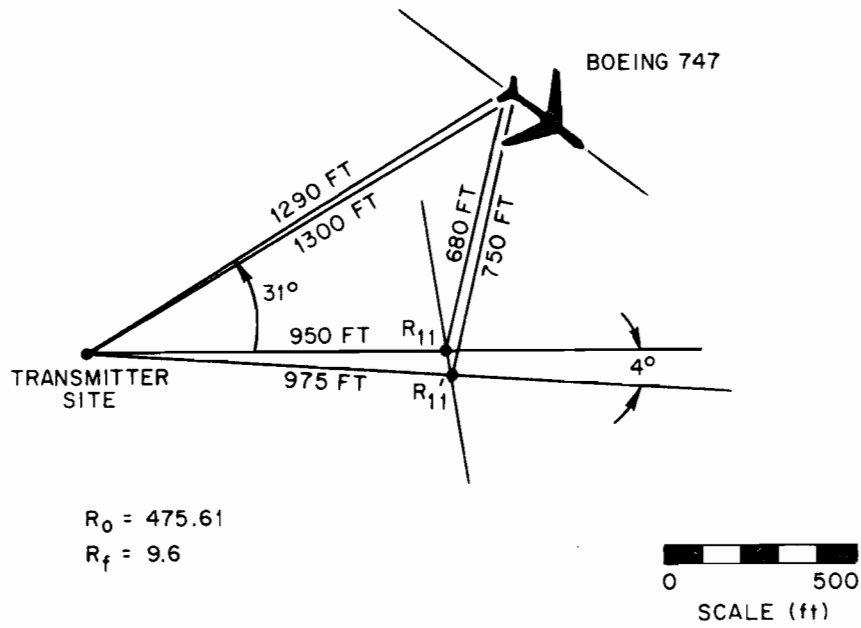


Fig. 34 Geometry for 11 December 1974 Boeing 747 experiment.

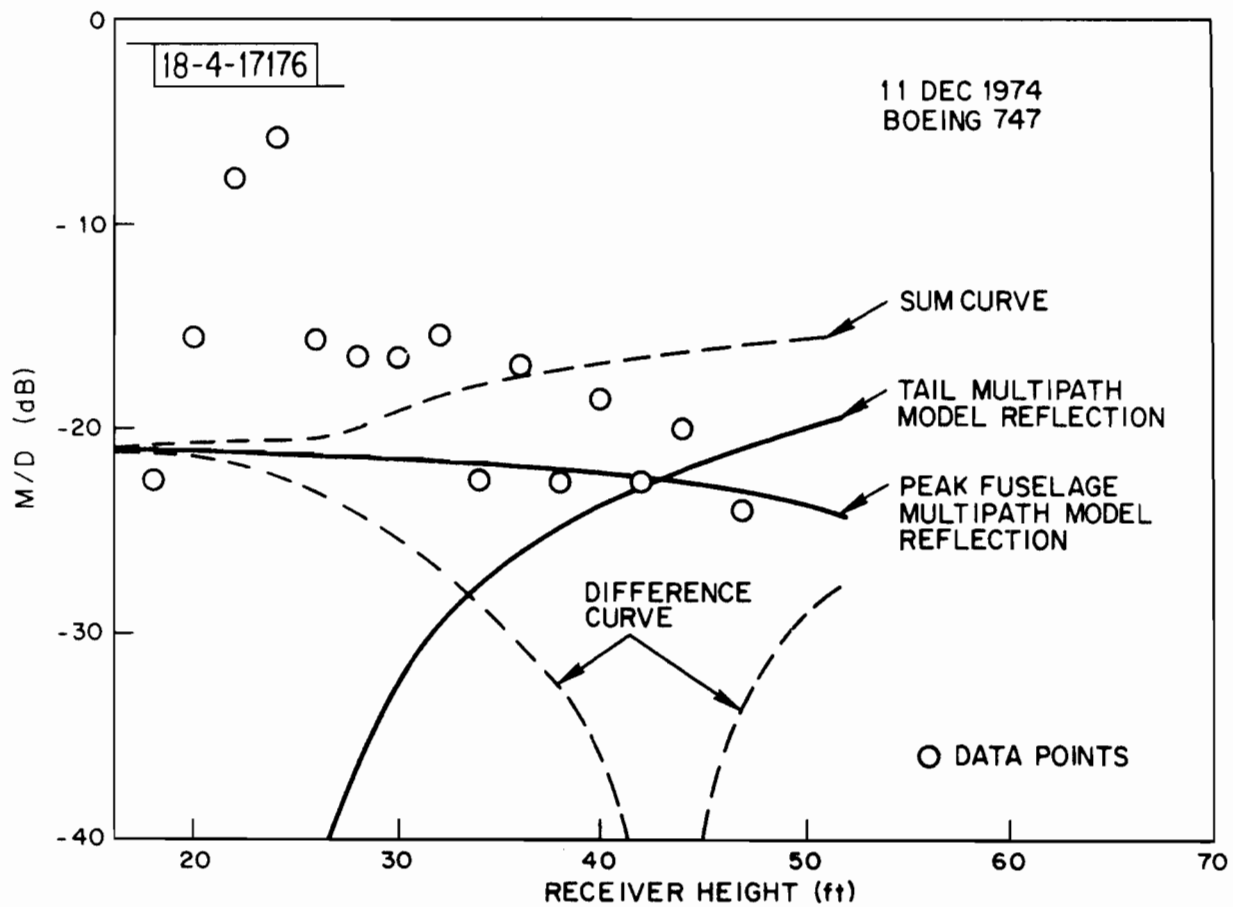


Fig. 35 Comparison of 11 December 1974 data with B747 multipath model M/D results.



Fig. 36 Boeing 727 airplane.

1974, reflection levels were measured from a parked Eastern B727 located near the Eastern hangar (see Fig. 30).

The geometry for the B727 data is presented in Fig. 37 where two receiver locations are shown. For the first,  $R_0$ , reflection off the front of the fuselage was observed to be about -23 dB. At  $R_0'$ , where the geometry is set up corresponding to reflection of the tail, data were obtained and are shown in Fig. 38 along with the model results. The peak in the data is assumed to be due to the engine pod in the B727 tail. As with the B747 data, the tail reflections occur well above the physical height of the tail due to the slight tilt in the tail. This was compensated for in Fig. 38 by exaggerating the tail height. Alternatively, the model could be modified to include the tilt, in which case the height exaggeration would be dropped. As is the case with the B747, the tail reflections dominate over the fuselage and the former are reasonably matched to the model.

### 5.6.3 Aircraft Data Summary

It was found that, for the geometries encountered, the tail was the main source of multipath reflection. The wings are not suitably oriented to cause reflections for MLS, and the fuselage is doubly curved in the front and rear and is shadowed by wings and engines in the center. The tail is large, oriented for reflections, relatively flat; and because it is angled slightly upward and is slightly curved, it generates reflections over large angles in space. The original model overestimated in both level and extent the reflections from the fuselage and underestimated the vertical extent of the tail reflections. By exaggerating the tail height, by choosing the largest tail fin length, and by decreasing slightly the fuselage length, better agreement between measurement and model are achieved. Alternatively, one could tilt the tail of the model instead of exaggerating its height. Model fuselage M/D levels were generally higher than those observed but this is acceptable because: (1) the measurements were at geometries\* at which more wing blockage occurs than

---

\*In particular, the restricted range of receiver heights.

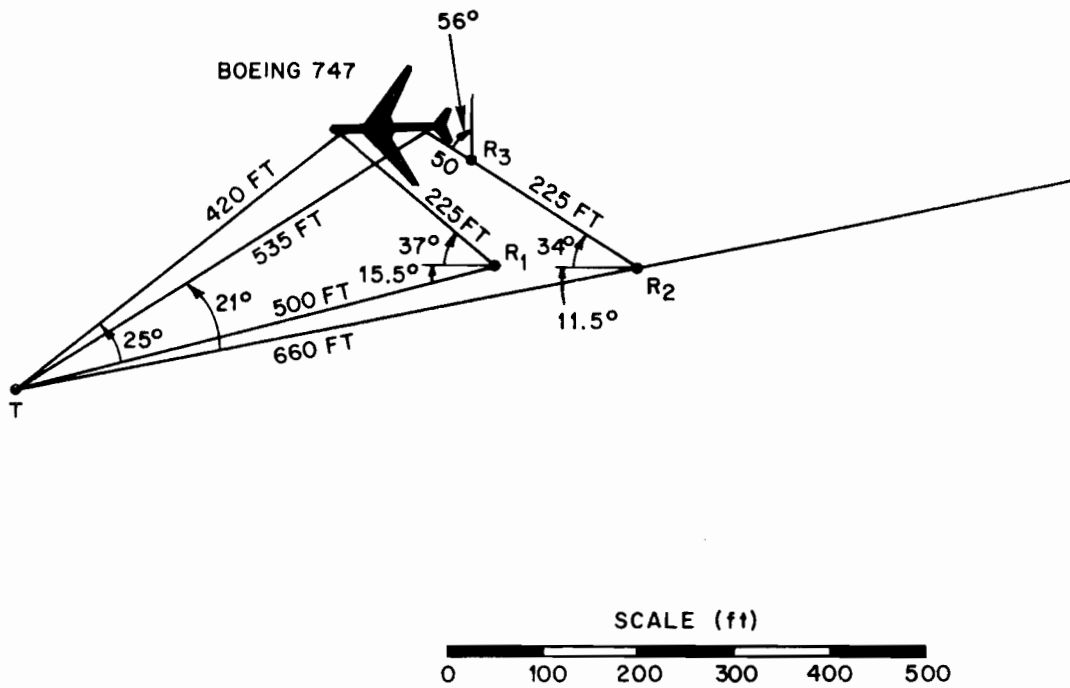


Fig. 37 Geometry for 12 December 1974 Boeing 727 experiment.

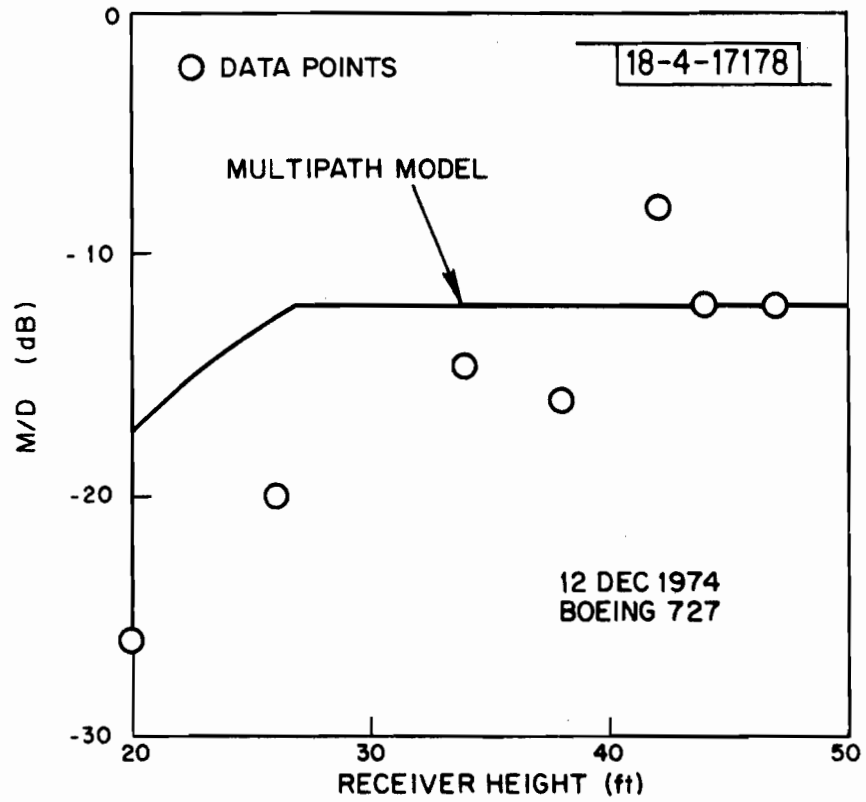


Fig. 38 Comparison of 12 December 1974 data with B727 multipath model M/D results.

in more realistic scenarios, (2) it was felt that a cylinder model for fuselages is very reasonable physically, and (3) it is better for the model to err on the high side than the low.

## 5.7 Ground Reflections

Ground reflections can obviously play a significant role in determining  $M/D$ <sup>[10]</sup> as is seen from (1). They affect both the direct signal and the reflected signal. If their effect is to be accounted, one must be able to characterize the ground as to its reflection coefficient,  $\rho_{RC}$ , its roughness, its flatness, and its slopes. Since this is at best a very tedious task, it behooved us to take pains to avoid these reflections in obtaining  $M/D$  data to characterize building reflections.

One cannot totally ignore ground reflections from an airplane fuselage since the cylindrical shape dispenses energy downward and we expect a ground reflection between the fuselage and the receiver.

The data obtained for ground reflections such as that cited in Section 4.2, behaved as expected.

### 5.7.1 Lobing From Ground Reflections

In Section 4.2, we saw that the lobing pattern of a mast run could be used to check the separation between the transmitter and receiver. A similar situation, on the morning of 18 October 1974 on runway 4R-22L, allowed us to compare geometry and reflection coefficient (as determined from the data) to estimates. The transmitter (see Fig. 11) was located near the threshold of runway 22L. The receiver was located, according to runway markings, 800 feet from the transmitter and a height run performed. The cw results, as recorded on a strip chart, are shown in Fig. 39. Adjacent nulls are at 19 feet and 10.5 feet so  $\Delta H = 8.5$  feet which corresponds to an  $r_0$  of

$$r_0 = \frac{2h(\Delta H)}{\lambda} = 814 \text{ feet} .$$

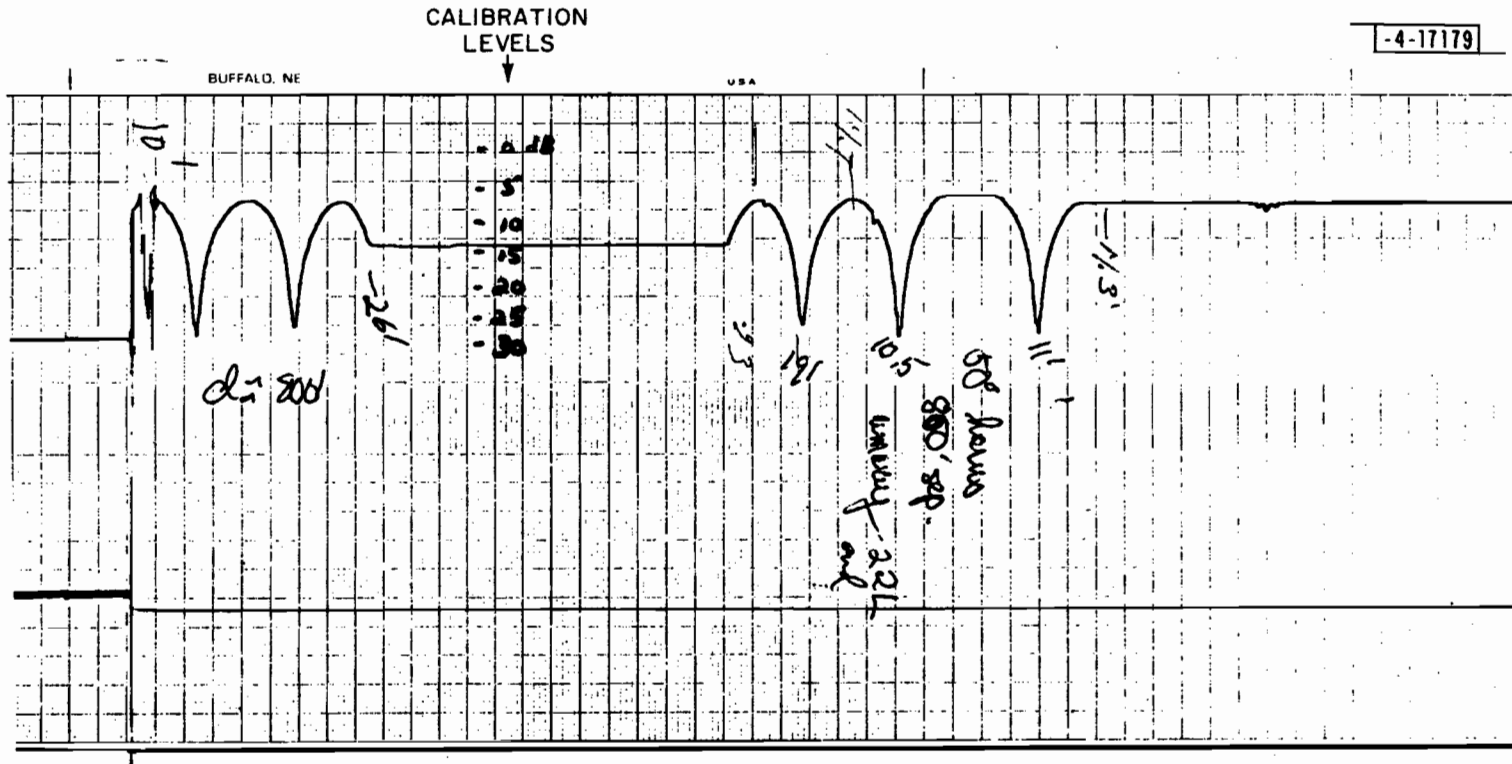


Fig. 39 cw strip chart from 18 October 1974.

The difference in level between peak and null is about 22 dB. This converts into a reflection coefficient of

$$\rho_{RC} = -0.85 \quad .$$

The grazing angle of the reflection is about  $2^\circ$ . The theoretical reflection coefficient for dry earth ( $\frac{\epsilon}{\epsilon_0} = 10$ ,  $\sigma = .001$  mhos/meter) is 0.8.

#### 5.7.2 Ground Reflection and Aircraft Lobing

DC-10 data were taken on the evening of 24 October 1974 with the cooperation of American Airlines. This pulsed data was not processed except for a single-peak reflection level of -29 dB averaged over a short receiver path run. There were multiple reflections from the airplane, some direct and others via ground bounce resulting in a highly scalloped cw strip chart.

The cylinder model under investigation for aircraft fuselage predicts a multipath component from the transmitter to the fuselage to the ground to the receiver. This particular component is of interest for elevation systems since the component has a positive angle code (roughly that of the fuselage center), yet involves a ground reflection. Similarly, during measurements of fuselage scattering, this component cannot be made negligible by using a transmitter antenna with sharp elevation cutoff. Thus, it was very difficult to experimentally measure its level.

However, there was indirect evidence as to its existence during the DC-10 measurements indicated above. With the transmitter antenna pointing at the fuselage (from a distance of 1000 feet and at an angle of  $29^\circ$ ), a vertical pole test was made with the receiver 360 feet from the fuselage reflection point. A lobing of peak-to-peak amplitude 3-dB and, spatial period of 2 feet were observed. The model predicts this two bounce component will have a level  $\rho_g$  with respect to the single-bounce fuselage reflection and a spatial wavelength

$$\Delta H = \frac{r_2^2 \lambda}{2h_f} = \frac{(360)(.2)}{2.(20)} = 1.8 \text{ feet}$$

where  $h_f$  is the fuselage height. This is quite consistent if we take the effective ground reflection coefficient for the grass between the taxiways to be 0.15 at  $9.45^\circ$  angle of incidence.\* Similarly, during a horizontal run parallel to the DC-10 fuselage axis through the same region with a receiver height at 40 feet, a 4-dB lobing was observed with a lateral period of 16 feet. The model predicts the lateral spatial period of

$$\delta = \frac{r_2^2 \lambda}{2 h_f H \cos \theta_i} = \frac{(320)^2(0.2)}{(2)(20)(40)(.87)} = 14.71 \text{ feet}$$

which agrees fairly well with the observed data.

To summarize, there is indirect evidence that the two bounce multipath from transmitter to fuselage to ground to receiver was present during at least one set of measurements. Its level was fairly low, probably due to the fairly sharp angle of incidence on the ground for the particular measurement geometry.

Similarly, for data obtained on 25 October 1974 on a Boeing 747, the receiver was moving and the cw data recorded on a strip chart. These data are highly and irregularly scalloped. The geometry is the same as for the DC-10 and is shown in Fig. 40. The receiver antenna was at 50 feet and the transmitter aimed at the tail. A sample of the B747 data, in which runway lights were used as references, is presented in Fig. 41. The lights were about 103 feet apart. Near light #2 we would expect a scalloping period between direct and aircraft reflection of about 1.5 feet expanding to about 3.5 feet near light #7. The actual scalloping is more complicated than that. Near light #2 there is a coarse scalloping of about 5 feet on top of which a one-foot scalloping appears. This is probably a combination of direct, tail-reflecting fuselage reflection and ground via fuselage reflection. Next to light #5, there is only one irregular scalloping with average period of about 3 feet. Since the measured

---

\*This suggests a roughness factor of  $\sigma_h \approx 0.03$  feet.

18-4-17180

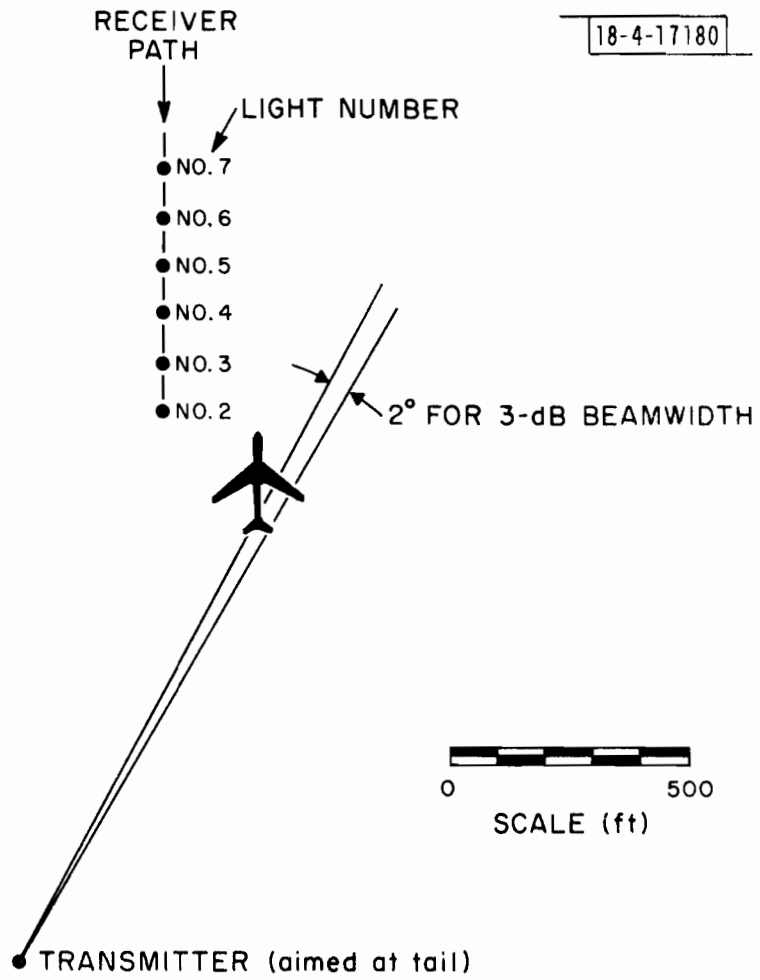


Fig. 40 Geometry for 25 October 1974 B747 experiment.

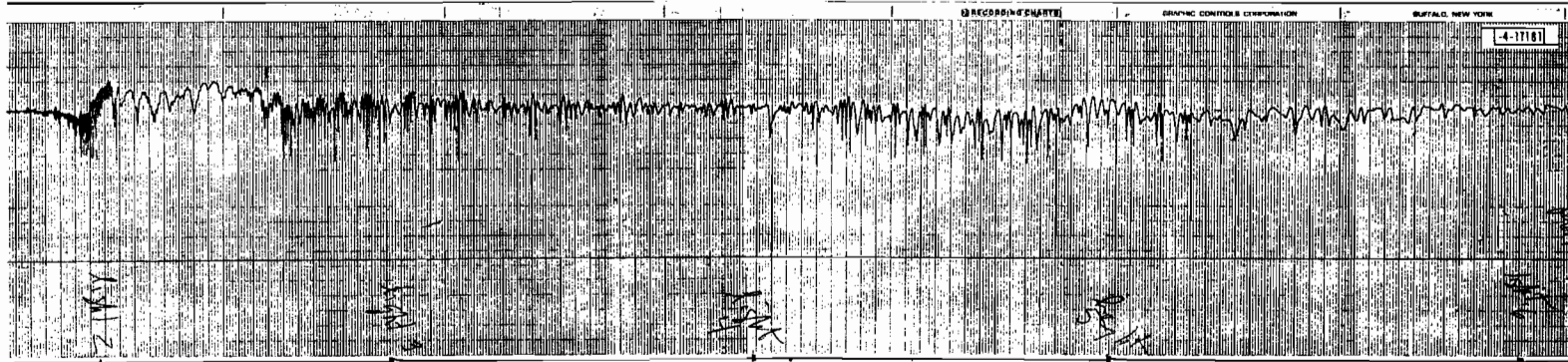


Fig. 41 cw strip chart from 25 October 1974 B747 experiment.

results are very complicated, it is difficult to draw any conclusions regarding which reflections are contributing to these results.

## VI DISCRIMINATION BETWEEN DOPPLER AND SCANNING BEAM MLS\*

An initial objective of the measurement program described here was to determine if discrimination between the two principal MLS techniques, Doppler scan and scanning beam, could be developed on the basis of the on-runway "realistic geometry" multipath data. The multipath features of interest are described in detail in a paper [11]; below we give a short summary:

- (a) Very high level azimuthal specular reflections: would suggest a possible need for coverage control and/or variable power programming with azimuthal angle [e.g., the hopover proposed for frequency reference scanning beam (FRS)] to avoid tracker failures.
- (b) Fading of cw reference: would suggest problems for function id and auxiliary data of Doppler and time reference scanning beam (TRS) as well as Doppler angle data reference
- (c) Moderate to high level elevation inbeam multipath; would suggest a need for substantial motion averaging as in Doppler and TRSB signal formats
- (d) Moderate to high level azimuthal multipath sum signal: suggests problems for Doppler system not using a tracking filter for signal acquisition.

For (a), one is concerned about levels that are above -4 dB as measured with a narrow azimuth beamwidth whose slope at the horizon is  $\approx 6$  dB/degree. However, no such levels were encountered in realistic on-runway locations using the parabolic reflector with either pulse or cw signals.

To assess (b), we consider the data using the cw signal and the broad beam antenna patterns. No substantial fades were observed that did not correspond to specular ground reflections (when near the transmitter) or blockage by a taxiing aircraft, although the antenna used had a vertical rolloff significantly less than contemplated for MLS omni-radiation.

---

\*This section was contributed by J. E. Evans.

There was moderate inbeam elevation multipath, but its level was not so high as to generate significant errors for Doppler or TRSB. However, an FRS system might experience appreciable errors ( $\approx 0.08^\circ$  rms) at the measurement site.

In the on-runway "realistic geometries," there were rarely more than two azimuthal specular reflections present at any one time and the sum level was always less than unity. Consequently, Doppler signal acquisition based on an unfiltered angle estimate would probably be successful. On the other hand, the levels were such that excessive errors might be encountered using a Doppler system without narrowband filtering, once signal acquisition had been accomplished.

To summarize, although there was no evidence that the on-runway "realistic geometry" measurements could be used as a discriminant between Doppler and TRSB, there would be a possible discriminant against the FRS technique on the grounds of poor inbeam elevation multipath performance.

## VII. CONCLUSIONS

It was established that the location of all important building reflections could be determined by modeling the buildings by simple flat plates and using geometrical optics and diffraction theory. Although other reflections occur, they apparently are so far below the direct levels that they can be readily ignored and, in fact, were not large enough to be measured in our experiment. Buildings, therefore, could be classified into two categories, complicated and simple. Complicated buildings, such as most terminal buildings, appear to be modelable by a single plate with a reflection coefficient commensurate with peak measured levels. Simple buildings, such as hangars, can be modeled by one or two plates whose reflection coefficients are determined by the dielectric and roughness properties of the surface construction material.

Aircraft reflections are more complicated because of the multitude of curved surfaces involved. The result is that there is no single number which tends to characterize reflections as is the case with many buildings. In addition, it is more difficult to judge the angular extent of the reflections and one is more dependent on the model for determination of the range of the reflection and the level for any particular geometry. There remain some principles which we can state. For airplanes on the ground, their tail reflections tend to dominate over other reflections for a couple of reasons. First, for the geometries that are likely to be found between the transmitter, airplane, and receiver, the tail is curved and oriented for reflections over a wider variety of situations. Second, fuselage reflections are often shadowed by the wings.

Good agreement between the model and experiment results was noted. There are some deficiencies in the airplane model due to the necessary simplicity of the model, but the resulting discrepancies should not be important. The utility of the model in helping to categorize and understand data from experiments and in extrapolating to new situations is obvious.

Finally, the on-runway "realistic geometry" measurements did not, of themselves, suggest a discriminant between the TRSB and Doppler techniques.

## REFERENCES

1. J. Capon, "Description of Computer Programs to Determine Obstacle Multipath Effects for MLS Simulation," Lincoln Laboratory, M.I.T. (to be published).
2. R.W. Hubbard, L.E. Pratt, and W.J. Hartman, "The Measurement of Microwave Multipath in an Airport Environment," Office of Telecommunications Report, U.S. Department of Commerce, Boulder, Colorado (to be published).
3. M.I. Skolnik, Radar Handbook (McGraw-Hill, New York, 1970), pp. 20-18 to 20-22.
4. R. P. Crow, "Summary of MLS DME Options," Informal memo (April 1975).
5. Texas Instruments MLS Phase II Report.
6. H. J. Riblet and C. G. Barker, "A General Divergence Formula," J. Appl. Phys. 19, 63-70 (1948).
7. D.E. Kerr, Propagation of Short Radio Waves, M.I.T. Radiation Laboratory Series 1951 (McGraw-Hill, New York; also Dover, New York, 1965).
8. Final Report of the Doppler Working Group to the MLS Technique Assessment Group (December 1974).
9. S. Sussman and R. S. Orr, "Validation of MLS Angle Receiver Simulation Models," Lincoln Laboratory, M.I.T. (to be published).
10. G. B. Litchford, "Study and Analysis of SC-117; National and USAF Plans for a New Landing System," USAF Flight Dynamics Laboratory Report AFFDL-TR-72-76 (July 1972).
11. J. E. Evans, private communications.

## REFERENCES

1. J. Capon, "Description of Computer Programs to Determine Obstacle Multipath Effects for MLS Simulation," Lincoln Laboratory, M.I.T. (to be published).
2. R.W. Hubbard, L.E. Pratt, and W.J. Hartman, "The Measurement of Microwave Multipath in an Airport Environment," Office of Telecommunications Report, U.S. Department of Commerce, Boulder, Colorado (to be published).
3. M.I. Skolnik, Radar Handbook (McGraw-Hill, New York, 1970), pp. 20-18 to 20-22.
4. R. P. Crow, "Summary of MLS DME Options," Informal memo (April 1975).
5. Texas Instruments MLS Phase II Report.
6. H. J. Riblet and C. G. Barker, "A General Divergence Formula," J. Appl. Phys. 19, 63-70 (1948).
7. D.E. Kerr, Propagation of Short Radio Waves, M.I.T. Radiation Laboratory Series 1951 (McGraw-Hill, New York; also Dover, New York, 1965).
8. Final Report of the Doppler Working Group to the MLS Technique Assessment Group (December 1974).
9. S. Sussman and R. S. Orr, "Validation of MLS Angle Receiver Simulation Models," Lincoln Laboratory, M.I.T. (to be published).
10. G. B. Litchford, "Study and Analysis of SC-117; National and USAF Plans for a New Landing System," USAF Flight Dynamics Laboratory Report AFFDL-TR-72-76 (July 1972).
11. J. E. Evans, private communications.